Abstract

Harris, Robert Bryan. Evaluation of Perfluoropolyether Coatings for Environmental Protection of Stone. (Under the direction of Dr. Richard D. Gould)

The objective of this study was to develop and evaluate the rapid expansion of supercritical solutions (RESS) as an environmentally safe coating process. RESS allows formation of small particles or droplets of polymers dissolved in supercritical carbon dioxide (SC-CO_2), by rapidly expanding the supercritical solution through an expansion nozzle. Due to the abrupt pressure decrease to atmospheric pressure, very high super-saturation values can be achieved. Furthermore, as the pressure change travels at the speed of sound, uniform operating conditions are maintained within the solution and a large number of small nuclei are formed. Previous RESS experimental results indicate it is an extremely attractive technology; small droplets and particles can be obtained with a narrow (mono-disperse) droplet size distribution. The present work is aimed at gaining an understanding of the relationship between droplet and spray characteristics and RESS process conditions. This was also extended to the evaluation of coating effectiveness at different RESS process conditions. Sandstone samples were coated with a perfluoropolymer (UNC diamide) by the RESS process for this study. The characteristics studied were transfer efficiency, liquid water contact angles, liquid water absorption and water vapor diffusivity.

The experimental results show that increases in process (i.e. supercritical solution) temperature reduce transfer efficiency. Increases in polymer coating thickness lead to higher contact angles, higher reduction of liquid water absorption and reduction in

water vapor diffusivity.

The synthesis of new polymers to be used for stone coating applications was also considered. The polymers designed and synthesized for this investigation were EVE (15)-ba and EVE (15)-au. Both polymers are derivatives of the same base polymer with the only difference being the pendent functionality. Therefore, these two new polymers contain multiple pendent functionalities per chain so they are capable of forming associative networks via hydrogen-bonding interactions that can result as an important factor in the water absorption data. This work presents the performance of these compounds brush coated on sandstone. The evaluation was based on performance of these compounds exposed to de-ionized water. Contact angle, liquid water absorption and water transport rates were measured for varying amounts of polymer coating.

Since the RESS process requires a large amount of polymer to be synthesized, therefore small-scale brush coating evaluations were used technique to identify coating compounds which display good water protection characteristics. The experimental data shows that the coating compound EVE (15)-au exhibited lower water absorption and also lower water vapor transport rate than the EVE (15)-ba coating. Finally, it was observed that there was not a significant reduction in water vapor transport as a result of the brush coating process with either compound. Identifying how pendent functionality affects coating properties is an important factor in developing a compound we wish to study by RESS process coating.

Evaluation of Perfluoropolyether Coatings for Environmental Protection of Stone

By

Robert Bryan Harris

A thesis submitted to the Graduate Faculty of
North Carolina State University
in partial fulfillment of the
requirements for the Degree of
Master of Science

Mechanical Engineering

Raleigh

2002

Approved by:

Chair of Advisory Committee

Biography

I was born April 30, 1977 in Burlington, North Carolina to Charles and Betty Harris. At the age of four, my family moved to Hillsborough, North Carolina, where I was raised and went to high school. I began attending North Carolina State University in the fall of 1995, majoring in Aerospace Engineering. As an undergraduate, I was group leader of my classes' senior design project. We were given the task of designing, constructing and flying a remotely piloted jet aircraft. I entered the graduate school at North Carolina State University in the fall of 1999, majoring in mechanical engineering. I began working on this project January of 2000.

Acknowledgments

I would like to thank Dr. Richard Gould for working with me on this project as well as advising my graduate studies. I would also like to thank several members of the Kenan Center for the Utilization of CO2 in Manufacturing, Dr. Ruben Carbonell, Dr. Yury Chernyak and Dr. Gerardo Montero, for their guidance and assistance. My thanks also extended to Dr. Jack Edwards and Dr. Michael Shearer for serving as committee members.

Table of Contents

List of Tables

List of Figures

Nomenclature

T_c	=	Cloudpoint temperature (^oC)
P_c	=	Cloudpoint pressure (psi)
T_{pump}	=	Temperature of ISCO pump (K)
P_{pump}	=	Pressure of ISCO pump (psi)
V_{pump}	=	Volume of ISCO pump (psi)
T_{exp}	=	Pre-expansion temperature (^oC)
P_{exp}	=	Pre-expansion pressure (psi)
Dv(50)	=	Average particle size distribution (μm)
D[3][2]	=	Sauter mean diameter (μm)
C_v	=	Volume concentration (PPM)
$T_{process}$	=	RESS process temperature (^oC)
m_0	=	Mass initial (g)
m_1	=	Mass initial (g)
wt%	=	Weight percent of polymer in solution (%)
M_w	=	Molecular weight
ρ	=	Density (g/m^3)
TE	=	Transfer efficiency (%)
W_{adh}	=	Wetting adhesion (dyn/cm)
γ_{LV}	=	Surface tension liquid at vapor interface (dyn/cm)
$\ominus$	=	Contact angle (degrees)
h	=	Height (cm)

ε_v	=	Porosity (%)
g	=	Gravitational constant (m/s^2)
PE	=	Protective efficacy (%)
RH	=	Relative humidity (%)
J	=	Molar flux
D_{eff}	=	Effective diffusivity
A	=	Cross sectional area (cm^2)
L	=	Length (cm)
R	=	Universal gas constant (J/(g·mol·K))
δ	=	Penetration depth (cm)
D_k	=	Diffusion coefficient
D_m	=	Molecular diffusion coefficient

1. Introduction

Highly fluorinated polymers have been shown to be ideal coatings for the protection of historical buildings and monumental civil infrastructure from stone degradation processes. [1,2]Low molecular weight perfluoropolyethers and the amides of their carboxylic acids, such as isobutyl amide and ethylene or hexamethylene diamides, are liquids at room temperature and have many physical properties that are favorable to the protection of porous surfaces. [3,4] These polymers are highly water repellent[5], have low surface energies and are stable to corrosive acids, high temperatures, UV radiation, and oxidizing agents. [6] Perfluoropolyethers are insoluble in water, transparent, and colorless. Moreover, they have a refractive index near that of water, meaning that the natural appearance of the stone can be maintained after coating. [7]

Perfluoropolymers are generally insoluble in most common solvents except for volatile organic compounds (VOCs) and fluorinated solvents. Ironically, VOCs and fluorinated solvents required to deliver coating materials to protect substrates from environmental degradation themselves can have a contaminating effect on the environment. A number of recent studies have focused on finding an alternative to the use of conventional organic and fluorinated solvents in order to give perfluoropolyethers a viable future as large-scale protective agents. It has been shown experimentally that fluorinated polymers and perfluoropolyethers in particular are highly soluble in CO_2. [8] Use of carbon dioxide as an alternative solvent has a number of advantages. It is environmentally benign, non-toxic, non-flammable, easily recyclable, and is a low cost,

widely available material. CO_2 has a relatively low critical temperature and moderate critical pressure ($T_c \approx 31\ ^oC$, $P_c \approx$ 72 bar). Thus, its supercritical state ($1<T/T_c<1.1$, $1<P/P_c<1.5$) [9] can be easily reached using conventional spraying equipment. In the supercritical state, the solvent properties of carbon dioxide are very sensitive to changes in the temperature and pressure. This gives access to a wide range of solvating strengths through controlling the process conditions. This versatility, coupled with environmental benefits, has led many industries to consider CO_2 as an alternative solvent.

The rapid expansion of supercritical solutions (RESS) process[10-25] is an environmentally benign alternative to conventional processes for producing fine droplets or powders. In this process, a dilute solution of a solute in a supercritical fluid (usually carbon dioxide) is expanded through a capillary nozzle from a high upstream pressure to a low downstream pressure. The resulting decompression leads to a high degree of super saturation of the solution with characteristic times for phase separation on the order of 10^{-5}-10^{-6} sec. [10-12] The precipitation of solute from the solution is driven by nucleation, condensation, and particle coagulation. The process can produce very small, nearly monodisperse particles or droplets, depending on the nature of the solute and the operating conditions. Figure 1.1 illustrates this process.

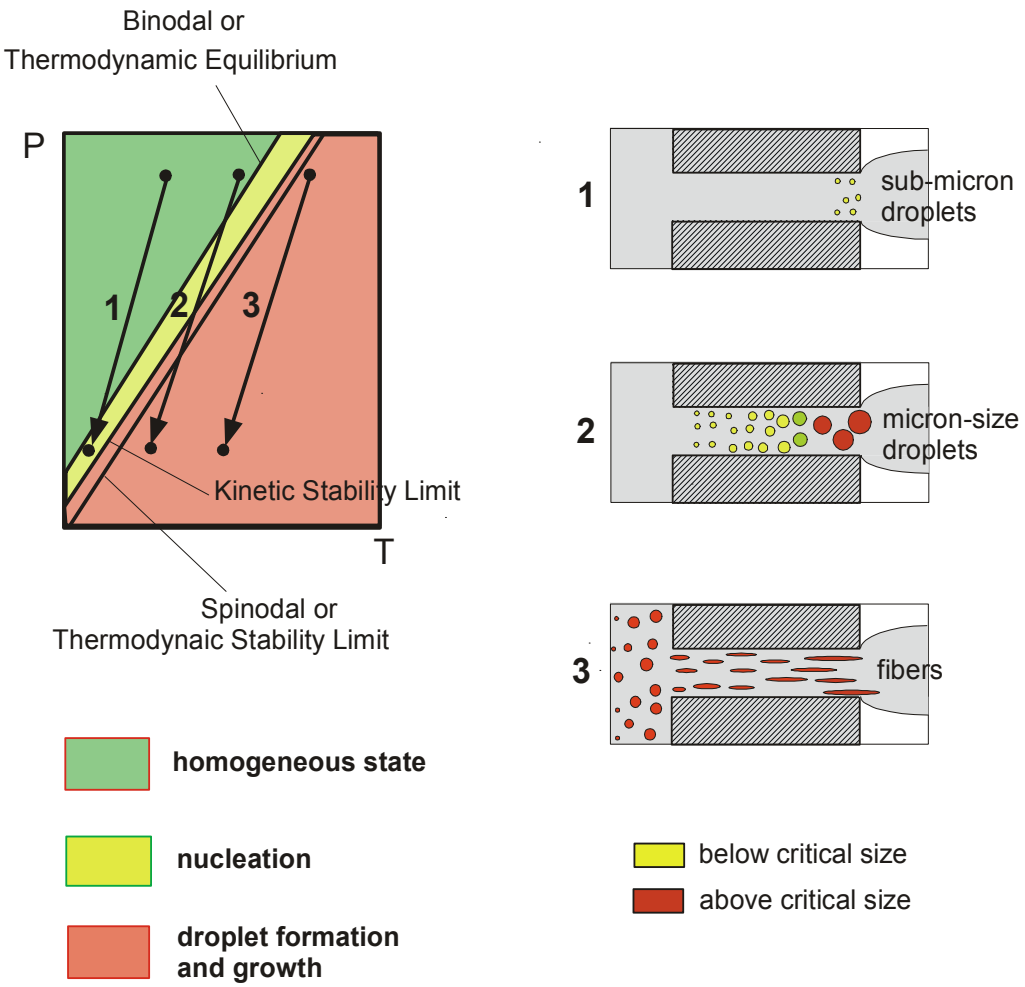

Figure 1.1: RESS droplet formation

The three cases represent three different RESS process paths from the entrance of the nozzle to the exit. The first case represents a solution that produces sub-micron particles. This case begins as a homogeneous solution and is expanded through the nozzle just crossing the bimodal equilibrium. Particles begin to nucleate from solution; however, the process of nucleation begins as the solution exits the nozzle. Once the solutions exits the nozzle particle growth is uncontrollable. The second case represents controllable particle formation and growth. Nucleation begins at the nozzle entrance.

The pressure drop across the nozzle transitions the solution into a spinodal region, where the solutions undergoes spontaneous phase decomposition. The nucleated particles now grow very quickly to form micron size particles. Upon exiting the nozzle further droplet growth through condensation and coagulation may occur. The coagulation mechanism is believed to play a key role in micron sized particle formation for the RESS process. [26] The third process path represents the formation of polymer tendrils. The solution has already crossed the cloud point curve and particles of critical size have formed upstream of the nozzle entrance. As the solution is expanded through the nozzle the polymer coalesces and fibers are drawn from the nozzle exit or the nozzle is plugged completely. This process of droplet growth is not controllable. In order to produce uniform particles by controllable means it is necessary to follow the second case process path.

The RESS process has attracted researchers hoping to overcome many of the issues facing the modern coatings industry. Initially, reduction of VOC emissions was the goal, but as the process developed, a number of other benefits were recognized. The RESS process is unique among the other spraying techniques due to its capacity for a wide range of organic, inorganic, polymeric and organometallic materials, its applicability to various substrates, and its ability to produce nearly uniform precipitates with different morphologies. [13,27] One disadvantage is that the process is limited to those materials that can be dissolved in the supercritical fluid. The possibility of controlling RESS product characteristics from sub-micron powders to super-micron fibers by varying operating conditions has been an active area of investigation since the late 1980s. [10,11,15-23,28] Most of these works are experimental in nature and are more descriptive rather than

predictive. Conclusions are generally limited to the specific material and process conditions studied.

Previous work focused on experimental efforts toward the analysis of RESS processing of a perfluoropolyether diamide (PFD) from its supercritical solution with carbon dioxide. [29] The intent was to achieve a more complete understanding of the processes that govern PFD droplet growth, with an eventual view toward predicting the effects of process conditions on droplet sizes and size distributions. Experimentally observed spray characteristics, such as droplet size distribution and transfer efficiency measurements have been documented. The effects of polymer concentration, pre-expansion temperature and pressure, on the spray characteristics were also described. It should be noted that the data is normalized to the cloudpoint temperature of the polymer solution. Normalized temperature is given by the following equation

$$T_N = T_{process} / T_{cloudpoint} \qquad (1.1)$$

The experimental and computational cloudpoint curves for the PFD[29] can be seen in figure 1.2.

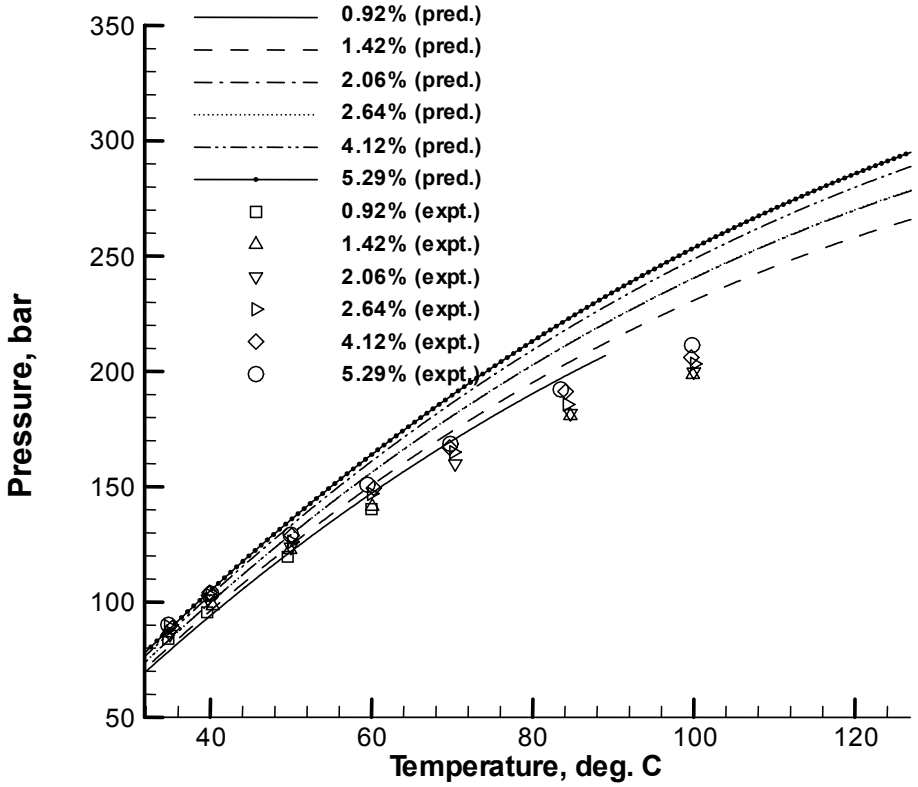

Figure 1.2: Experimental and predicted cloudpoint curves

Transfer efficiency measurements were also carried out for the PFD. The results of the previous work[29] are shown in figure 1.3.

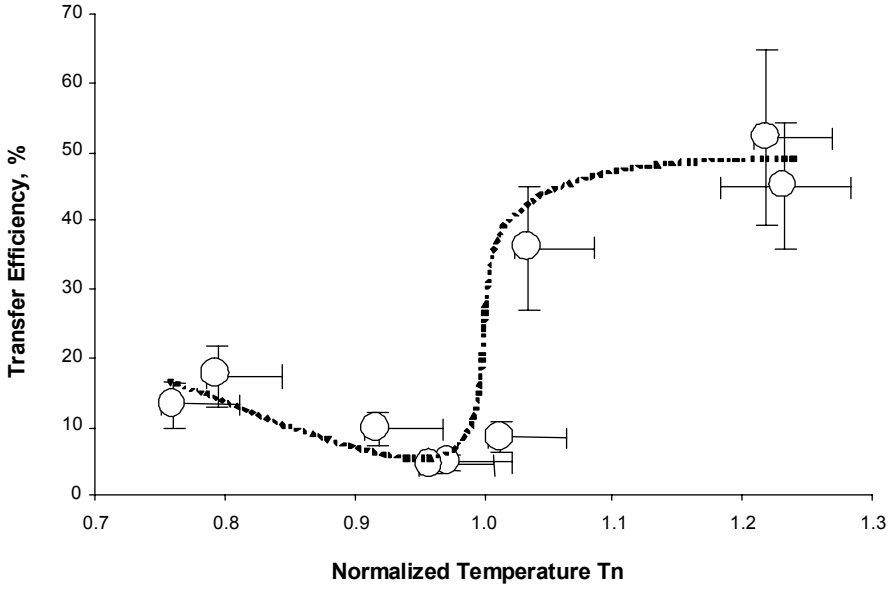

Figure 1.3: Transfer efficiency of PFD as a function of process temperature

Above the cloudpoint curve, as temperature increases the transfer efficiency decreases. As the process conditions cross the cloud point the transfer efficiency rapidly increases. However, the spray product is a coagulation of polymer tendrils. This phenomenon was observed during the transfer efficiency experimentation. This is undesirable as the polymer tendrils do not adhere to the surface of the stone and thus a protective coating is not obtained.

The data indicates that an increase in solution concentration and a decrease in pre-expansion temperature results in a narrowing of droplet size distribution as displayed in figure 1.4.

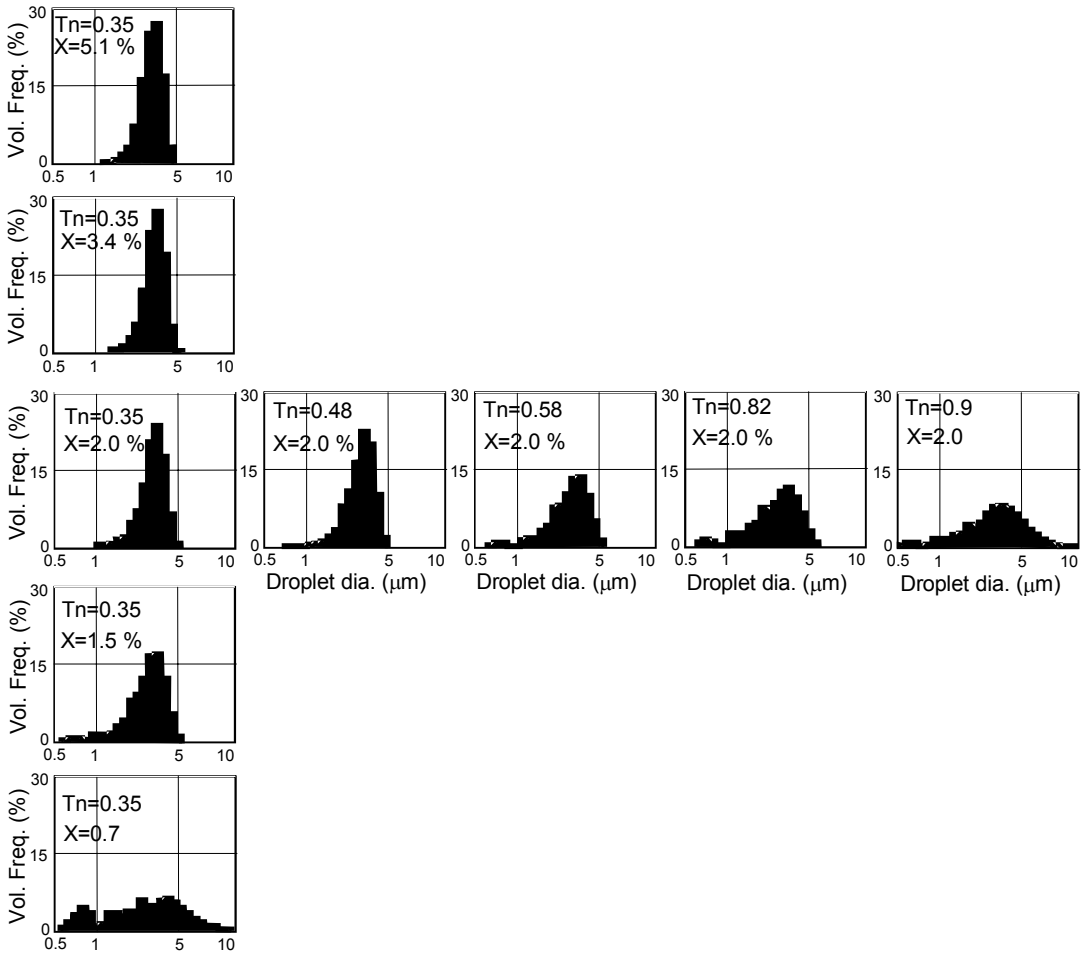

Figure 1.4: Droplet size distribution of PFD

The present work involves characterizing a polymer of similar structure with a higher molecular weight. In addition to this, the RESS process was evaluated for its protective coating ability. The evaluation was based on performance of these compounds coated on sandstone and exposed to de-ionized water. Contact angle, liquid water absorption and water transport rates were measured for varying RESS process conditions.

The synthesis of new polymers to be used for stone coating applications was also. The polymers designed and synthesized for this investigation were EVE(15)-ba and EVE(15)-au. Both of the polymers are derivatives of the same base polymer with the only difference being the pendent functionality. Therefore, these two new polymers contain multiple pendent functionalities per chain so they are capable of forming associative networks via hydrogen-bonding interactions that can result as an important factor in the water absorption data. This work presents the performance of these compounds brush coated on sandstone. The evaluation was based on performance of these compounds exposed to de-ionized water. Contact angle, liquid water absorption and water transport rates were measured for varying amounts of polymer coating.

2. Experimental Setup

A discussion of brush and spray coating techniques and spray coating techniques by the rapid expansion of supercritical solutions is given in section 2.1 and 2.2. Section 2.3 discusses the measurements of water droplet contact angles. The water absorption measurement technique is given in 2.4. Finally, section 2.5 describes the diffusivity measurement technique used in this study.

2.1 Brush Coating

One of the goals of this research was to evaluate new coating compounds. Often experimental compounds are expensive and very time consuming to synthesize. In addition to this, the experimental compounds were not specifically designed for spray coating. As such, brush coating is an effective way to apply limited amounts of polymer to stone surfaces. The following sections describe the materials and techniques used in the brush coating experiments.

2.1.1 Brush Coating Materials

The stones examined in this study were Pietra Serena sandstone. The samples used for the experiments were 1 cm thick with square cross section of 5 cm x 5 cm. All the samples of the same lithotype were taken from one large boulder, in order to minimize differences in physical properties. These samples were characterized by the

Italian National Research Center of Florence (CNR-C.S. Cause Deperimento e Metodi di Conservazione Opere d'Arte, Italy); the characteristics are reported in Table 2.1.1.1.

Table 2.1.1.1 Sandstone Properties

Stone type	**Pietra Serena Sandstone**
Chemical Composition	32 % Quartz 21 % Calcium carbonate 13 % Plagioclasi 7 % Ortoclasio 7 % Dolomite 20 % Other
Pore radius (μm)	0.3 +/- 0.1
Porosity (%)	9.2 +/- 0.2

The perflouropolyether (PFPE) compounds designed and synthesized by the Chemistry department at UNC-Ch, for the brush coating investigation were EVE(15)-ba and EVE(15)-au. Their structures are given in following figure.

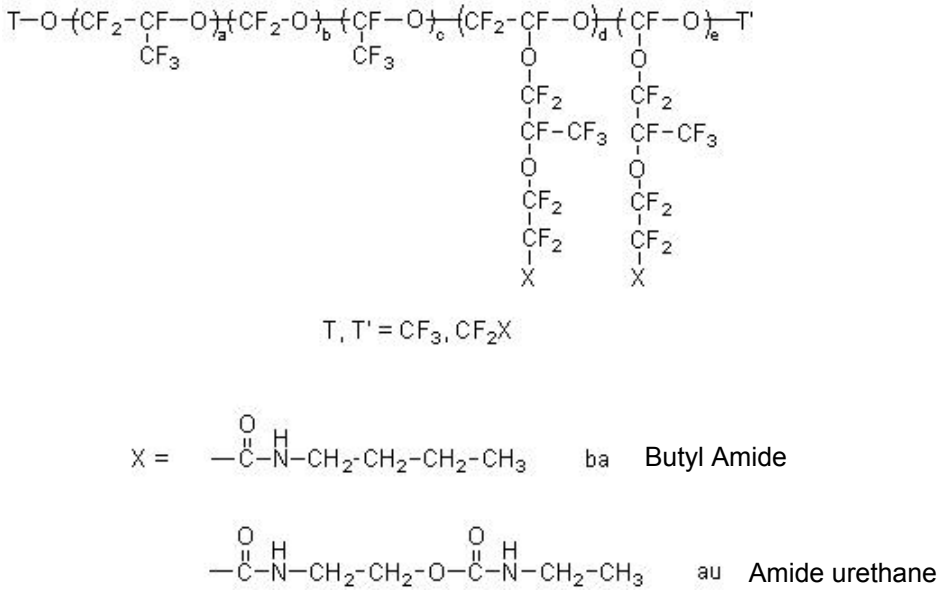

Figure 2.1.1.1: Chemical structures of PFPE compounds

Both of the polymers are derivatives of the same base polymer and the only difference is the pendent functionality. Therefore, these two polymers contain multiple pendent functionalities per chain so they are capable of forming associative networks via hydrogen-bonding interactions that can result in an important factor in water absorption behavior. These are soluble in organic solvents such as acetone and are liquid at room temperature and pressure. [30]

2.1.2 Brush Coating Procedure

To begin brush coating for a particular stone, a desired amount of polymer is chosen. Freon was used as the primary solvent for the brush application of PFPE's. A small glass specimen container is placed on a balance and the reading is zeroed. An amount of polymer is weighed out into the container. Then Freon is added until the polymer in the container is completely dissolved. If Freon does not completely dissolve the polymer acetone is mixed in as well. As the solvents are added their weight and volume are recorded. The mass of each component of the solution is known and therefore the weight percent of polymer can be calculated from the following equation.

$$wt\% = {m_{solute}}/{m_{solution}} \times 100 \qquad (2.1.2.1)$$

Knowing the weight percent gives the mass of solution required to apply a desired mass of polymer.

$$m_{solution} = {m_{polymer}}/{wt\%} \qquad (2.1.2.2)$$

The volume needed to apply the desired mass of polymer is now calculated. Since the amount of polymer in the solution is relatively small it is assumed that the volume of the polymer is negligible compared to that of the solvent. Thus, the density of the solution is assumed to be that of the solvent. The volume for a given coverage is calculated from the following equation.

$$V_{desired} = m_{solution} / \rho_{solvent} \qquad (2.1.2.3)$$

This volume of solution can now be applied to the stone. The stone samples are kept in an incubator at 50 ºC. In order to record accurately the amount of polymer delivered to the surface the stones are weighed before and after coating. Stones are first examined for surface imperfections, such as cracks and chips. The surface which has the least amount of imperfections is the side chosen for coating. The stone is then numbered with the side to be coated oriented upward. Uncoated stones are removed from the incubator and placed in a desiccator for 1 hour. This allows the stones to cool to room temperature. The uncoated stone is then removed from the desiccator and placed on a balance and the weight is recorded. This process is repeated once a day, until three consecutive readings are within 0.01 grams deviation. After each weighing the stones are placed back in the desiccator. The stone's weights fluctuate depending on the humidity of the atmosphere. It is not possible to keep the stones completely dry, therefore the weight is averaged over three readings to get an accurate estimate of weight. After the average weight is found coating can be applied. When the coating solution is prepared the uncoated stones are taken from the incubator and placed in the desiccator for 1 hour, the stones are then taken from the desiccator and polymer is applied. The calculated volume of solution is then placed into a glass specimen container. The solution is then brushed onto the surface until the container is empty. Once the polymer solution has been applied to the stone, it is placed in the incubator to allow the solvent to evaporate leaving only the polymer. The stone is weighed once a day until three consecutive readings are approximately the same.

The amount of polymer applied to the stone can then be found by subtracting the weight before coating from that after coating.

2.2 Rapid Expansion of Supercritical Solutions (RESS)

The other main goal of this work was aimed at gaining an understanding of the relationship between droplet and spray characteristics and RESS process conditions. This also included the evaluation the coating effectiveness at different RESS process conditions. Sandstone samples were coated with a perfluoropolymer by the RESS process in this part of the study. The characteristics studied were transfer efficiency, liquid water contact angles, liquid water absorption and water vapor diffusivity. The following sections describe the materials and techniques used in the RESS coating experiments.

2.2.1 RESS Coating Materials

The stones used in the RESS coating experiments were from the same lot as those used in the brush coating study. The characteristics of Pietra Serena sandstone are given in table 2.1.1.1

Solutions of a 3600 M_w perfluoropolyether diamide (PFD) in CO_2 were used in this work for the experimental study and theoretical modeling of the RESS process. This polymer has the following chemical structure. For the purposes of this investigation this polymer will be referred to as UNC diamide

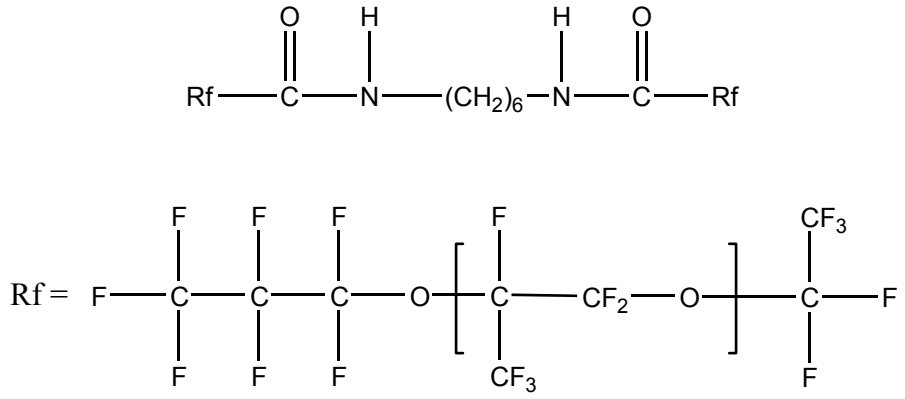

Figure 2.2.1.1: Chemical structure of UNC diamide

The UNC diamide is a liquid at ambient conditions. Supercritical solutions were formed with carbon dioxide of bone-dry grade (99.8% minimum purity) supplied by National Welders Co. The physical properties of CO_2 are well known. [31]

2.2.2 Solubility Measurements

The phase equilibrium apparatus used in this study is shown in figure 2.2.2.1.

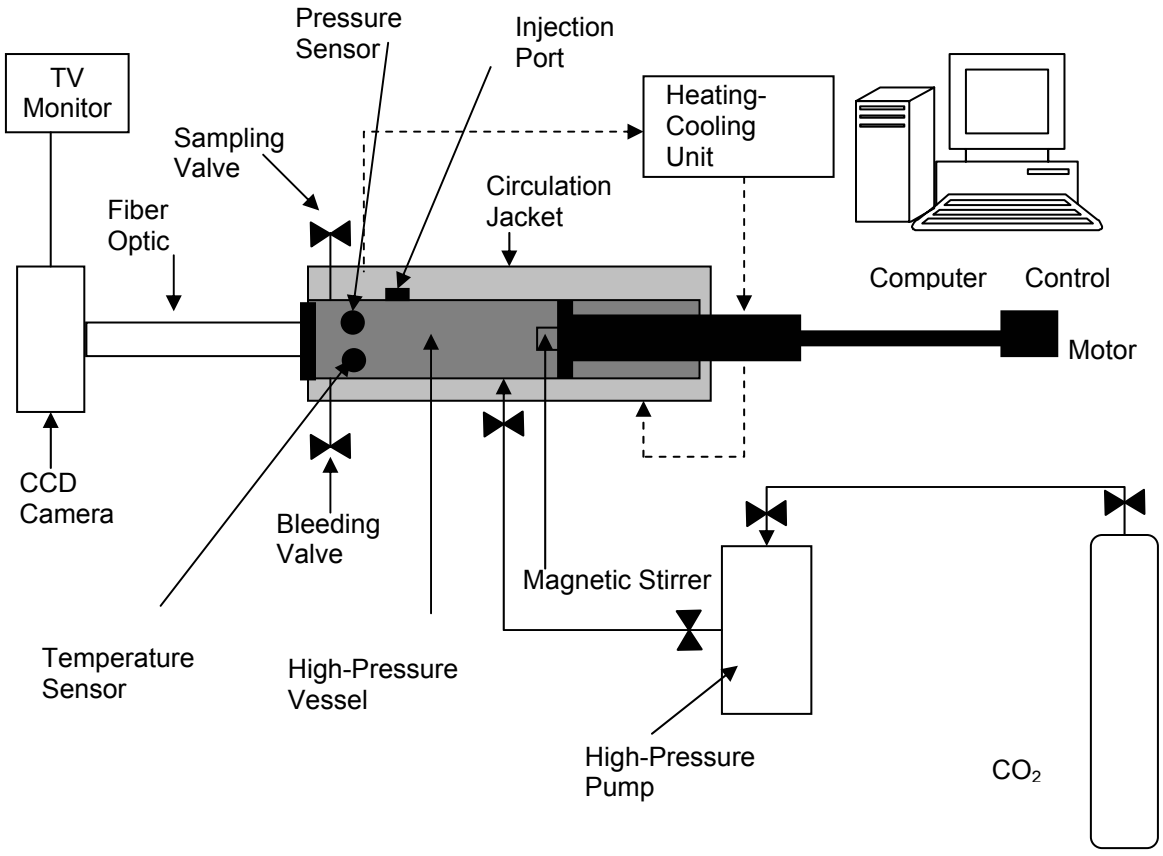

Figure 2.2.2.1: Thar designs phase equilibrium apparatus

Cloud point pressures were typically measured three times at constant temperature and composition to minimize operator error. For a given concentration and temperature, the pressure in the cell is raised such that the polymer / CO_2 solution begins to form a single phase. At this point the pressure is further increased until a completely homogeneous phase is present. Once this has been achieved the pressure is gradually lowered such that

phase separation begins. The equilibrium condition is defined to be the pressure at which opalescence (cloudiness) in the solution is first observed as the pressure is lowered. These measurements were reproducible within ± 3% (i.e. ±90 psi at 3000 psi) at each temperature and composition. Experimental data were taken first at a lower temperature and then at a higher temperature.

2.2.3 RESS Experimental Setup

The rapid expansion of supercritical solutions (RESS) experimental setup used for spray coating in this work is shown schematically in figure 2.2.3.1.

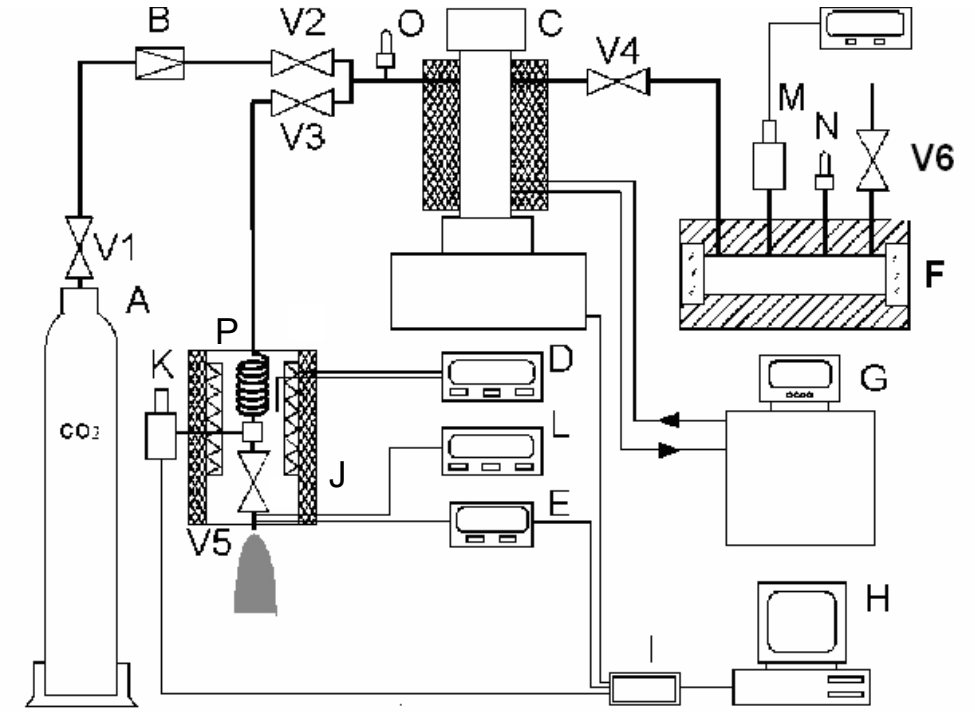

Figure 2.2.3.1: RESS experimental setup

It consists of three major units: a high-pressure stainless steel view cell (F) with sapphire windows, an ISCO 260D syringe pump (C) and a pre-expansion unit (J). A solution of polymer in CO_2 is prepared gravimetrically at ambient temperature in the view cell. The pressure of CO_2 in the cell is set above the solubility limit. When the polymer is dissolved in the cell, the solution is transferred into the syringe pump. The polymer/CO_2 solution is then pressurized by the syringe pump and is heated to the desired starting

process conditions (P_{pump} and T_{pump}). The temperature of the solution in the syringe pump is regulated by circulating a water/ethylene glycol mixture from the thermostated bath (G). Before the solution leaves the nozzle, it is pumped at pressure P_{pump} to the pre-expansion unit and is heated isobarically to the pre-expansion temperature (T_{exp}) by passing it through the heated coil leading to the nozzle. The supercritical solution is allowed to expand to ambient pressure through the nozzle. Temperatures in the pre-expansion unit and in the nozzle are controlled by Omega CN76000 temperature controllers (D) and (L) and are maintained constant to within 3 K during the solution expansion. The pressure and temperature of the polymer/CO_2 solution are measured upstream of the nozzle orifice by an Omega PX302-10KGV pressure transducer (K) and a K-type thermocouple with uncertainties of 1 bar and 0.8 K, respectively. All measured parameters (i.e. pressure and temperature of the flow, and flow rate) are recorded during the spraying process. The typical amount of polymer solution in the pump is between 100-150 ml, which is sufficient for up to 3-4 min of spraying time at the selected operating conditions. A feature of this apparatus is its ability to control independently the temperature in the bulk part of the solution (T_{pump}) and that prior to entering the nozzle (T_{exp}) while maintaining a constant solution concentration. This allows one to set a desired process path and to correlate RESS product characteristics with the operating conditions. A detailed RESS operational procedure can be found in Appendix 6.1

2.2.4 RESS System Nozzle Configuration

The nozzle configuration used in this work is shown in figure 2.2.4.1. The nozzle assembly consists of a capillary tube of 25mm length with an outer diameter of 1/16" and an inner diameter of 0.006". The capillary tube is held in place by a pressure fit gland and sleeve. The components of the nozzle were purchased from High Pressure Equipment (HiP), their part numbers are included in figure 2.2.4.1.

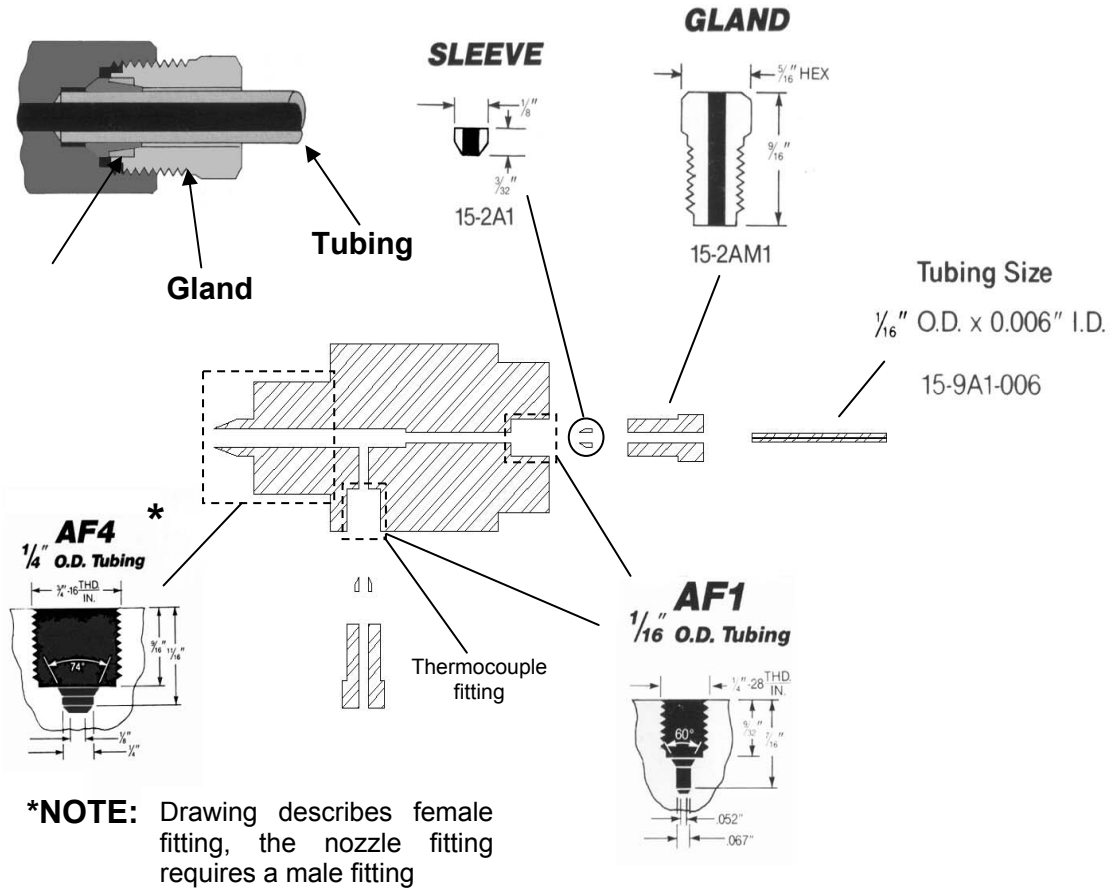

Figure 2.2.4.1: Nozzle configuration

It was necessary to machine a fitting to accept the nozzle and the thermocouple. Technical drawings of the interior geometry and the machined fitting can be found in figure 2.2.4.2. The dimensions are given in English units, which is the standard used in North Carolina State University machine shops.

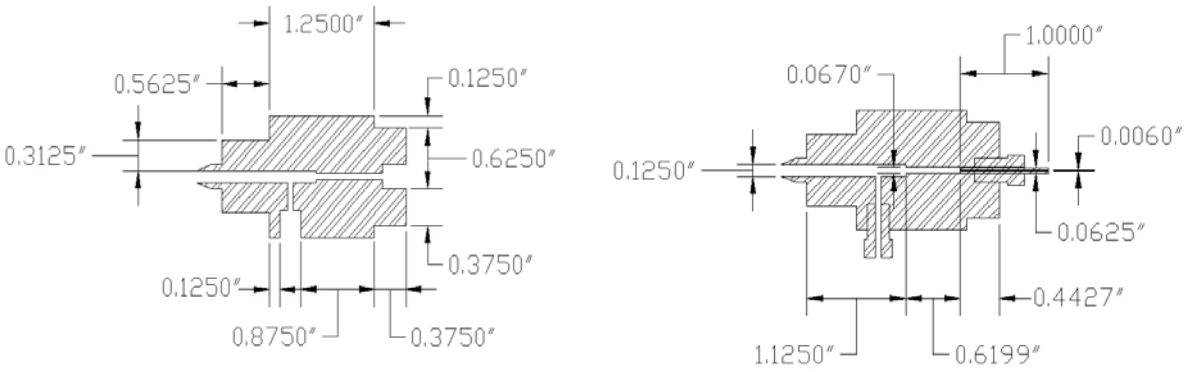

Figure 2.2.4.2: Nozzle fitting dimensions

2.2.5 RESS Spray System Particle Sizing

Most RESS spray characterizations described in the literature have been performed via off-line techniques. This is because most materials processed by RESS to date were solids at ambient conditions. In our experiments, droplet characterization has been performed on-line using a non-intrusive laser technique based on Fraunhofer diffraction. A Malvern Spraytec Model RTS 5006 droplet sizing system capable of measuring particle diameters between 0.5 and 200 μm was used. The instrument consists of a transmitter unit, which produces a horizontally-oriented collimated laser beam, and an in-line receiver unit separated by approximately 300 mm. The spray is directed downward through this beam between the transmitter and receiver units. The instrument measures the light scattered from the droplets passing through the laser beam at various angles using a solid-state ring detector located in the forward scattering direction. A graphical representation can be seen in figure 2.2.5.1.

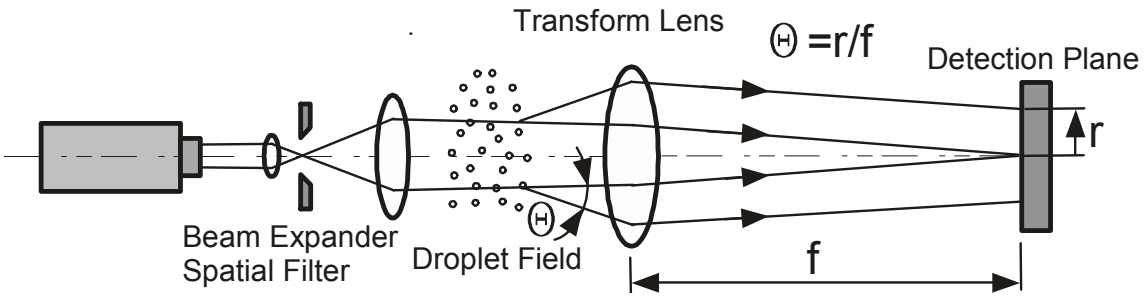

Figure 2.2.5.1: Laser diffraction particle sizing instrument

The accompanying software calculates the droplet size distribution necessary to produce the measured scattered light energy. Droplet size distribution (volume frequency vs. diameter), the diameters at 10% (Dv10), 50% (Dv50) and 90% (Dv90) the cumulative volume, the Sauter mean diameter (D[32]), the distribution span, and the percent light transmission through the spray are output. Measurements reported in this work were taken 152 mm downstream of the nozzle exit plane. A detailed operating procedure for online measurement can be found in Appendix 6.2

2.2.6 Spray Coating Methodology

Once the UNC diamide was characterized by determining cloud point and droplet size measurements at various operating conditions, spray coating was begun. The first performance measure of RESS spray coating examined was transfer efficiency.

Polymer transfer efficiency (TE) measurements were performed by spraying a PFD/CO_2 solution through the 150 μm ID, 25 mm length capillary nozzle onto a 5x5 cm sandstone substrate placed at a distance 5 cm from the nozzle exit. The measurements were performed for a solution of 2 wt% of PFD at 140 bars (2000 psi) and 165 bars (2400 psi) at various pre-expansion temperatures. The transfer efficiency is defined as the mass of PFD present on the substrate after coating divided by the initial mass of PFD in the solution and is expressed as a percentage value. The mass of PFD on the substrate was measured by weighing the stone sample before and after coating. Preparation of the RESS system involved the following steps. A predetermined amount of polymer is chosen. To produce a 2 wt% solution approximately 4.7 g of polymer is required. This is because the RESS system consistently begins with approximately 230 ml of CO_2 at 10 C and 4000 psi (V_{CO2}). The solution is prepared as described in Appendix 6.1. After the system has reached equilibrium the volume of the solution in the ISCO pump is recorded, as well as the temperature and pressure. As per procedure, the valve between the ISCO pump and the nozzle is opened and the solution now fills the lines and the ISCO pump. This volume is recorded and denoted as V_{pump}. Once the system is set to the desired process conditions coating may begin. A sandstone substrate is removed from the incubator and placed in a desiccator for one hour. This is done so the temperature of the stone is cooled to room temperature. The stone is placed on a lab stand and positioned 5

cm from the nozzle exit. The entire bulk solution is then sprayed onto the stone. The coated stone is then placed in the incubator. The stone remains in the incubator until it appears to be dry. Depending on the amount of polymer deposited this may take anywhere from 1 day to 1 month. The stone is then weighed each day until a stable reading is reached. Prior to spray coating the stone's dry weight is measured. This again is an average taken from a minimum of three consecutive stable readings to obtain an accurate measurement. The amount of polymer deposited on the stone can now be calculated and thus the transfer efficiency can be calculated. The first step is to calculate the wt% of the solution. This is to check that the desired conditions for spraying are met.

$$wt\% = {m_{polymer}}/{(m_{CO_2} + m_{polymer})} \times 100 \qquad (2.2.6.1)$$

The mass of CO_2 is found from the following equation given the recorded volume of CO_2 at 4000psi and 10 C. The thermodynamic properties of CO_2 are well documented. For these calculations density properties were obtained from the NIST tables. [32]

$$m_{CO_2} = V_{CO_2} * \rho_{CO_2} \qquad (2.2.6.2)$$

Now the amount of polymer sprayed by the RESS device is calculated using,

$$m_{spray} = {(m_{polymer} + V_{pump})}/{V_{total}} \qquad (2.2.6.3)$$

Where $m_{polymer}$ and V_{pump} are known quantities and V_{total} is the total volume of the system CO_2 and polymer at the temperature and pressure of the system after it reaches equilibrium overnight.

The amount of polymer delivered to the stone is measured by subtracting the initial weight of the stone substrate before spraying from the weight of the stone after spraying. This is denoted as $m_{p\ stone}$.

$$m_{p\ stone} = m_{1\ stone} - m_{0\ stone} \tag{2.2.6.4}$$

Transfer efficiency is calculated from the following equation.

$$TE = {m_{p\ stone}}/{m_{spray}} \times 100 \tag{2.2.6.5}$$

2.3 Contact Angle Measurement Technique

The wetting of coated stones is an important factor of environmental protection. Wetting is defined as the process in which a fluid phase is displaced from the surface of a solid by another fluid phase. [33] Wetting, as a result of adhesion is given by the following equation.

$$W_{adh} = \gamma_{LV^\circ}(1 + \cos\theta) \tag{2.3.1}$$

Where W_{adh} is the work of adhesion, γ_{LV}° is the surface tension of water at an air interface (72.2dyn/cm) and θ is the contact angle of the liquid water droplet.

A surface is said to completely wet if the measured contact angle is 0º and completely non-wetting if the contact angle is 180º. However, in practice, contact angles of 180º are not attainable. It is widely accepted that contact angles equal to and above 90º are sufficient for non-wetting. [34] Figure 2.3.1 displays the geometric definition of a contact angle.

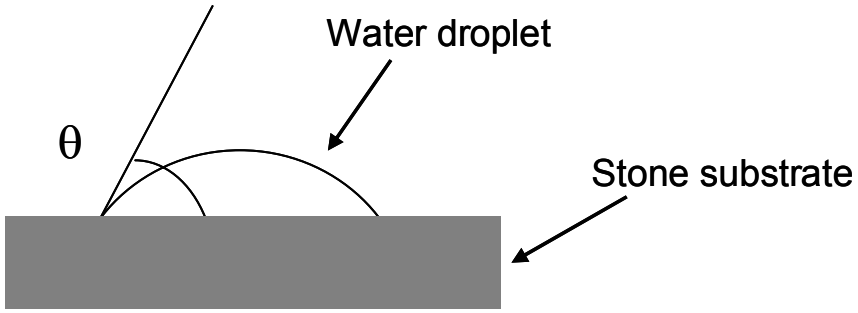

Figure 2.3.1 Contact angle measurement

Equation 2.9.1 shows that the value of W_{adh} is controlled by the contact angle. Determining the contact angle of water on coated stones provides the wettability. Measuring water contact angles on sandstone can prove difficult. The main obstacle is the porous nature of the sandstone. Liquid water droplets are readily absorbed by the stone. In order to deal with this issue a technique described by Kossen et al. was used. [35]This technique is based upon the property that as the volume of liquid droplet is increased it will reach a point where further increases in volume have no effect on the height of the droplet. Once a droplet which displays this property is placed on the stone surface, a contact angle calculation can be performed using the following equations.

$$\cos\theta = 1 - \sqrt{\frac{Bh^2}{3(1-\varepsilon_v)(1-Bh^2/2)}} \qquad (2.3.2)$$

$$B = \frac{\rho_L g}{2\gamma_{LV}} \tag{2.3.3}$$

Where h is the height of the droplet (cm), ε_ν is the porosity of sandstone substrate (0.092), ρ_L = density of liquid droplet (g/cm^3), g is the gravitational constant (cm/s^2) and γ_{LV° is surface tension of water at an air interface (72.2dyn/cm).

The droplet must be stable before it can be measured. Therefore, the sandstone is first saturated with liquid water. This prevents that droplet from being absorbed into the stone.

To begin the water droplet/coated stone experiments, the coated stones are saturated with de-ionized water. Then the water saturated stone is placed on water saturated filter paper in a dish. The dish is to prevent the stones from drying out during the experiment. The upper surface of the stone is wiped with a lint free cloth to remove excess water. It is important that enough water is removed from the surface of the stone so that it does not disrupt water droplets placed on the surface. The dish is placed on a stand that can be leveled about two degrees of freedom by using a small circular bubble level placed on the surface of the stone. A CCD camera is positioned next to the stand and is interfaced to a PC so that online frame capturing may be performed. The camera is leveled as well. This assures that the camera is observing the side view of the droplet. A light source was place above and slightly forward of the stand and a dark screen was placed behind the stand. This aided in observing the droplets. A diagram of the setup is given in figure 2.3.2.

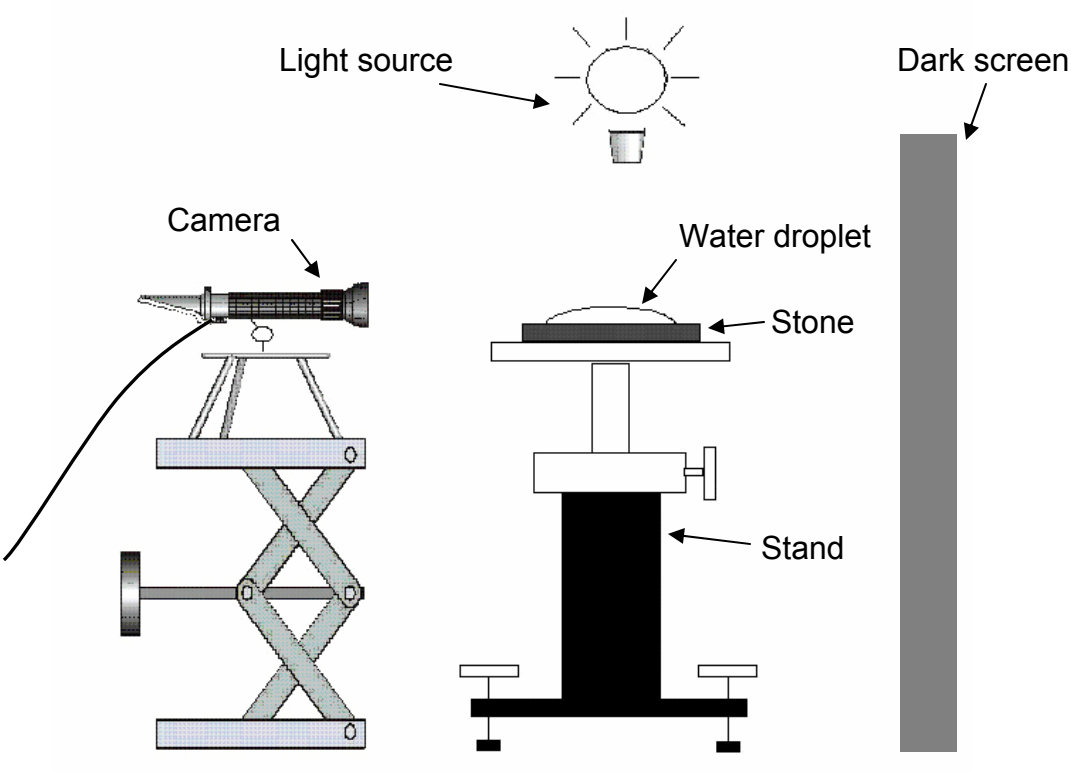

Figure 2.3.2: Contact angle apparatus

For each stone it is necessary to set a reference height that the camera observes. This is achieved by placing an object, of a known height, on the center of the stone. The object chosen was a small magnetic stirring bar, with a height of 5.2mm. Once the stone and the camera are leveled a still image is taken of the stirring bar on the surface of the stone. Once this reference image is taken the stone and the camera can not be moved for the remainder of the experiment. If the camera or the stand is moved during the experiment it would cause error to be introduced in the measurement of the droplet height. Now that the reference is set, and taking care not to disturb the instruments, a water droplet is placed on the surface by means of a syringe. For this system, 0.9 cc of de-ionized water produced a droplet that did not increase in height as volume was added. This droplet was

also small enough to reside on the stone surface. After the water is delivered to the surface the droplet is allowed to settle for approximately one minute. A still image is taken of the midsection of the droplet. This is the point at which the droplet height is most accurately recorded. In addition to the mid section, the two sides of the droplet are captured. The contact angle of each side is recorded and averaged. Despite careful leveling the stone surface it is still possible for the droplet to display hysteresis (i.e. advancing and receding sides of a droplet). For this reason, an average contact angle is taken from both sides. During the experiment a hystereisis larger than 5º was not observed. If that case were to occur, the measurement would have to be repeated. The images were then processed using the Deneba CANVAS© software package. An example of using CANVAS to determine contact angle is given in figure 2.3.3. This process is repeated for every stone.

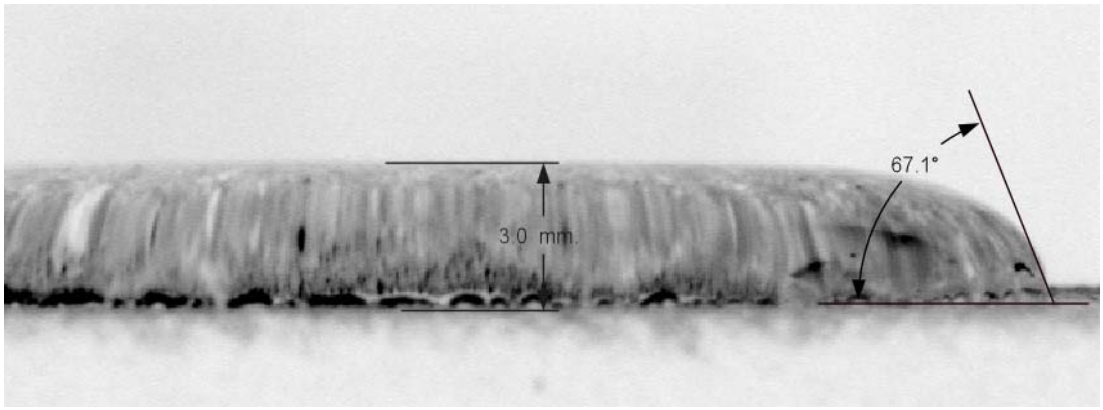

Figure 2.3.3: Water droplet on coated sandstone

2.4 Water Absorption Measurement Technique

The reduction in liquid water absorption due to a coating is sometimes defined as the "protective efficacy" of the polymeric material. This protective efficacy, PE, is defined as

$$PE = \frac{m_o - m_1}{m_o} \times 100\% \qquad (2.4.1)$$

where m_o and m_1 are, respectively, the mass of water absorbed by the sample before and after it has been coated.

The water absorption experiments start by choosing a set of stones for testing. Sandstone substrates 5 cm square and 1 cm thick were used. Each stone is examined and numbered. The surface that is to be coated is oriented number side up. The stones are stored in an incubator in order to keep them dry. In order to begin experimentation the stones dry weight must be determined. Each day the stones are removed from the incubator and placed in a dessicator for one hour. The stones are removed from the dessicator after 1 hour and weighed. The stones are then placed back into the dessicator. This process is repeated until three consecutive weight measurements are the same to within +/- 0.01 grams. The experiment consisted of placing stacks of 20 paper filters (9 cm diameter) in a glass baking dish, filled with approximately 1 cm of de-ionized water. The water level should be below the height of the stack of paper filters in order for them to wet by capillary absorption. The stone samples are taken from the incubator and placed in the desiccator for 1 hour. When the paper filters were completely damp, the stone samples were taken out of the desiccator, weighed and placed on a filter stack, the

face to be coated directly in contact with the saturated filter paper. The stones begin to absorb moisture immediately after being removed from the desiccator. In order to record accurate pre-wetting weights one stone is removed from the desiccator weighed and placed in the tray at a time. This is done in intervals of one minute. After one hour the sandstone samples were removed from the plastic tray, slightly dabbed with a saturated piece of lab tissue, and weighed again. This again is done at intervals of 1 minute for each stone. This ensures that the stones are exposed to the atmosphere and the water in the tray for approximately the same amount of time. The increase in stone weight corresponded to the water absorbed by capillary action. Each measurement was repeated at least three times with intervals of a couple of days, during which the samples were placed back in the oven at 50 ˚C. This was to allow the absorbed water to evaporate from the stone sample. This experiment was also repeated using the coated stone samples and the protective efficacy of the protective material was calculated.

2.5 Diffusivity Measurement Technique

The device used to measure the water vapor flux through the stone substrates is illustrated in figure 2.5.1

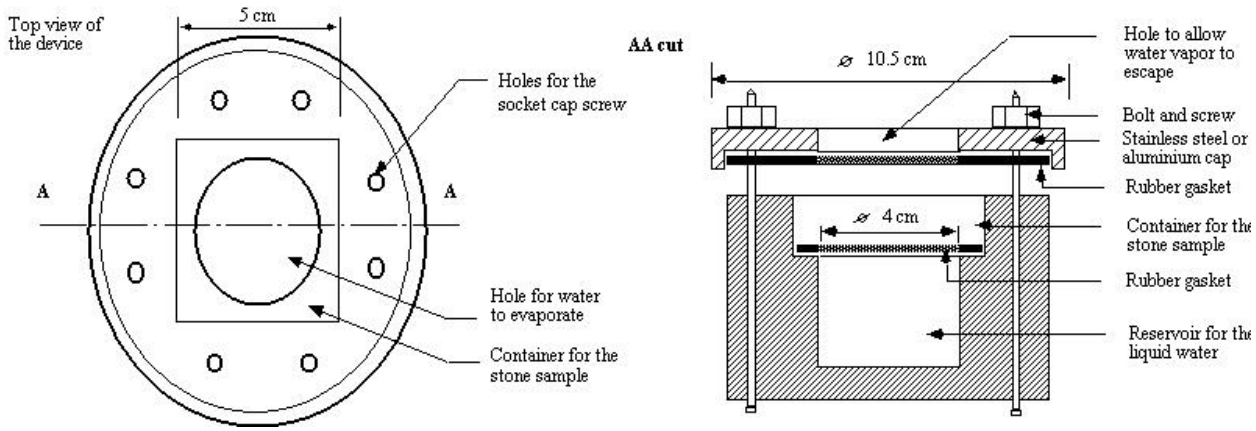

Figure 2.5.1: Diffusivity apparatus

The main body of this device consisted of a cylindrical Plexiglas cell of 10.5 cm outside diameter and 7 cm in height. A cylindrical reservoir 4 cm in diameter and 2.8 cm deep holds liquid water while a receptacle of 5 x 5 x 1.5 cm, carved directly above the reservoir holds the stone sample. A total of ten diffusivity apparatuses were constructed for experimentation. Rubber gaskets were placed under and above the stone to prevent bypassing of water vapor around the sample. The lid of the device was made out of oxidized aluminum, with a 4 cm diameter hole in the center, to allow the water contained in the reservoir to evaporate. The two sections of the device are tightened uniformly with bolts. The first step is to obtain diffusivity measurements of uncoated stones. Uncoated

sandstone substrates were stored in an incubator at 50 ºC until their weight stabilized. The stones are weighed each day until a stable weight is recorded for three consecutive days. The next step is to prepare the glove box for the experiment. The crucial aspect of this experiment is maintaining a low constant relative humidity. Diffusion is a concentration driven process, therefore the lower the ambient humidity (ie. glove box) the stones are exposed to, the higher the transfer rates will be. By doing this, any reduction in the diffusivity as a result of coating is more easily observed. The relative humidity (RH) of the air inside the glove box was kept low (RH of ~14 %) by distributing desiccant in several trays inside the environmental chamber. The box was insulated on all sides except for the glove door, to maintain a constant inside temperature of about 24˚C. A high precision balance (Mettler-Toledo-Model PR 1203) was also kept in the conditioned space. The uncoated set of stones are removed from the incubator and placed in a desiccator for 1 hour. This allows the stones to cool to room temperature. Each reservoir is filled with 30cc of de-ionized water and a stone is placed in each cell. The side of the stone to be coated is placed face down in the cell. The cell is then sealed and the bolts are tightened uniformly. In addition to stones, an aluminium block is placed in a cell. This is used to measure the bypass of water vapor around the seal. This is done because it is not possible to obtain a perfect seal. The bypass loss from the aluminium block is subtracted from stone diffusivity measurements to normalize the readings. The cells are then placed in the glove box. In order to seal the box further, packing tape is applied to the joints of the glove box door. The first weight recording is taken 24 hours after closing of the box. It is necessary to wait one day, since during loading the glove box is opened and the humidity inside is raised to that of the room value. The length of

this experiment was about three weeks during which time the weight of each cell was recorded daily. In addition to the weight loss, the temperature and humidity are monitored daily to ensure continuity of the system. The weight loss of a given cell corresponds to the amount of liquid water evaporated through the porous stone sample. The results are entered into Microsoft Excel®. At the completion of the experiment the stones are removed from canisters and placed in the incubator. The stones can then be coated with a perflouropolymer. Once the stones are coated the process is repeated. Once again the results are entered into Microsoft Excel® for interpretation.

The molar flux (J) of water vapor diffusing through the stone sample can be related to the rate of weight loss of the liquid water contained in the reservoir,

$$J = \frac{\text{moles}_{H_2 0}}{\text{Area} \cdot \text{time}} = -\frac{1}{A} \cdot \frac{1}{M_{H_2O}} \cdot \frac{dW_{H_2O}}{dt} \qquad (2.5.1)$$

Where W_{H2O} is the weight of water, M_{H20} is the molecular weight of water, and A is the area available for the diffusion process. The steady-state, local, one-dimensional diffusive flux of the solute in the x-direction in the sandstone is given by the following equation. [36,37]

$$J = -D_{eff} \frac{dc}{dx} = \text{constant} \qquad (2.5.2)$$

Substituting equation (2.5.1) into (2.5.2) gives equation (2.5.3) and allows the effective diffusivity (D_{eff}) to be found. In this work D_{eff} is $D_{0,eff}$ if the stone is uncoated, and $\bar{D}_{eff}$ if the sample has received a polymeric coating.

$$J = \frac{\text{moles}_{H_2 0}}{\text{Area} \cdot \text{time}} = -\frac{1}{A} \cdot \frac{1}{M_{H_2O}} \cdot \frac{dW_{H_2O}}{dt} = D_{\text{eff}} \left[\frac{c_1 - c_0}{L} \right] = \frac{D_{\text{eff}}}{RT} \left[\frac{p_1 - p_0}{L} \right] \quad (2.5.3)$$

Here the molar concentrations of solute are related to the partial pressures through the ideal gas equation of state. The quantities p_1 and p_0 are the partial pressures of water vapor inside and outside the cell, respectively, and are known parameters. The pressure p_1 is equal to 23.756 mmHg, corresponding to the pressure of saturated water vapor at the box average temperature of 25 ˚C, while p_0 is taken to be equal to 14 % of the saturated vapor pressure, due to the 14% relative humidity generally present in the glove box. The rate of loss of water in the reservoir, dW_{H20}/dt, which equals the weight loss of the whole cell, is obtained from the slope of the device mass curve with time (M_t/M_o vs. t). The penetration depth of the polymer inside the sandstone was then estimated from the experimentally determined values of $D_{0,\text{eff}}$ and $\bar{D}_{eff}$ following the technique described in previous research by Henon. [21]

The general equation relating the overall effective diffusivity to the local diffusivities is shown below.

$$\frac{D_{0,\text{eff}}}{\overline{D}_{\text{eff}}} = 1 + \left(\frac{\delta}{L} \right) \left[\left(\frac{1 + D_{K,1}/D_m}{1 + D_{K,0}/D_m} \right) \left(\frac{\varepsilon_0}{\varepsilon_1} \right)^{3/2} - 1 \right] \quad (2.5.4)$$

Where δ is the penetration depth of the polymer, L is the length of the sandstone in the direction of the mass flux, $D_{K,1}$ and $D_{K,0}$ are diffusion coefficients of the coated and uncoated stones, respectively, D_m is the molecular diffusion coefficient, and ε_0 and ε_1 are the porosity of the uncoated and coated stones, respectively. The length (L) and the porosities (ε_0) are properties of the stones. $D_{K,0}$ can be estimated by the expression, [38,39]

$$D_K = \frac{2}{3}\bar{r}\sqrt{\frac{8RT}{\pi M_{H_2O}}} \tag{2.5.5}$$

Where $\bar{r}$ the average pore radius of the sandstone, R is the universal gas constant, T is temperature, and M_{H20} is the molecular weight of water. The ratio of $\varepsilon_{1/}\ \varepsilon_0$ can be expressed as,

$$\frac{\varepsilon_1}{\varepsilon_0} = 1 - \frac{M_p/A}{\rho_p \delta \varepsilon_0} \tag{2.5.6}$$

Where M_p is the mass of the polymer applied, A is the area of the coated surface, and ρ_p is the density of the polymer. The polymer penetration depth can be found by substituting equation 2.5.6 into 2.5.4.

3. Results

Experimental measurements of contact angle, protective efficacy and water vapor diffusivity of polymer coated sandstone are given in this chapter. The first three sections give the brush coating results while the last four sections give spray coating results.

3.1 Brush Coating Contact Angle Measurements

Figure 3.1.1 shows the measured contact angles of liquid water droplets on the brush coated sandstone. The two methods of measurement, height calculations from equations and visual inspection, are displayed in this figure versus amount of polymer coating. Section 2.3 describes the experimental methodology of these methods.

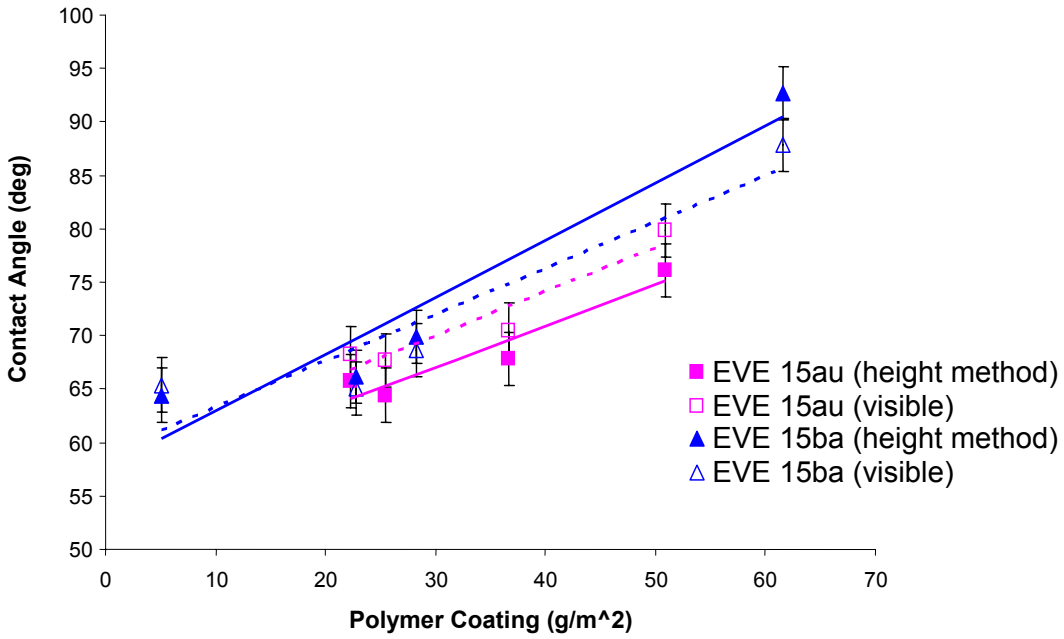

Figure 3.1.1: Contact angle measurements of brush coated sandstone

It can be seen that the two methods give contact angles to within five degrees of each other. This is a good check that the measurements are reasonably accurate. As expected the contact angles increase with a corresponding increase in polymer coating. It can be seen that the contact angle on the EVE 15au coated stones decreases slightly from the first coating thickness to the second coating thickness. This can be attributed to a difference is surface roughness between the stones, although the measurements are within the measurement uncertainty. The coatings only approached conditions of non-wetting, that is a contact angle greater than 90 degrees, when polymer coatings were approximately 65 g/m^2 for EVE 15ba. The maximum contact angle for EVE15au, roughly 75 degrees, was achieved at approximately 50 g/m^2. Due to the small amount of polymer available for experimentation, larger amounts of polymer were not applied to stones. In Figures 3.1.2 and 3.1.3 the effect of extended exposure to liquid water on contact angle are given for two coating magnitudes (i.e. thicknesses).

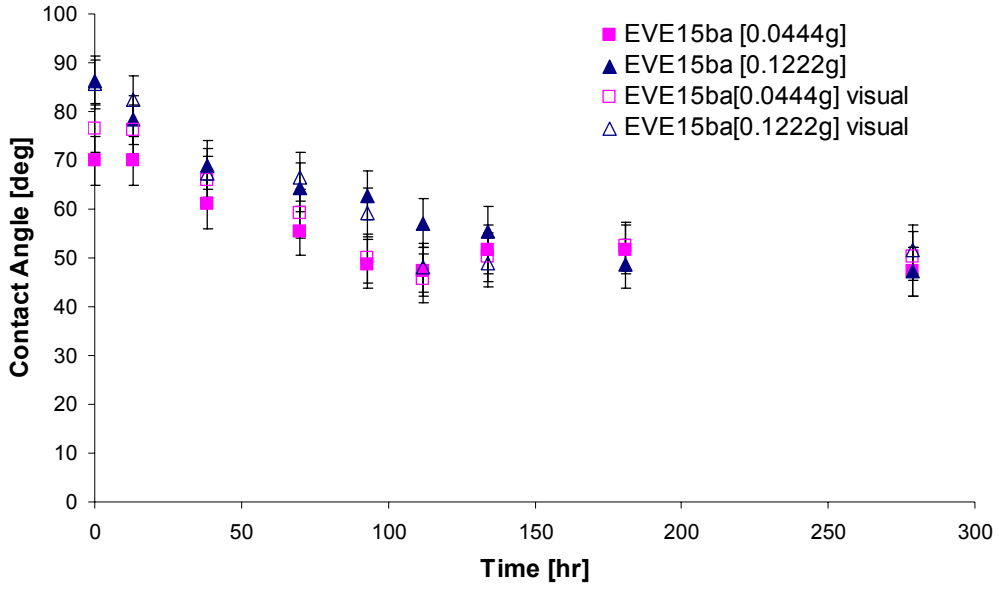

Figure 3.1.2: Contact angle versus time of EVE15ba brush coated sandstone

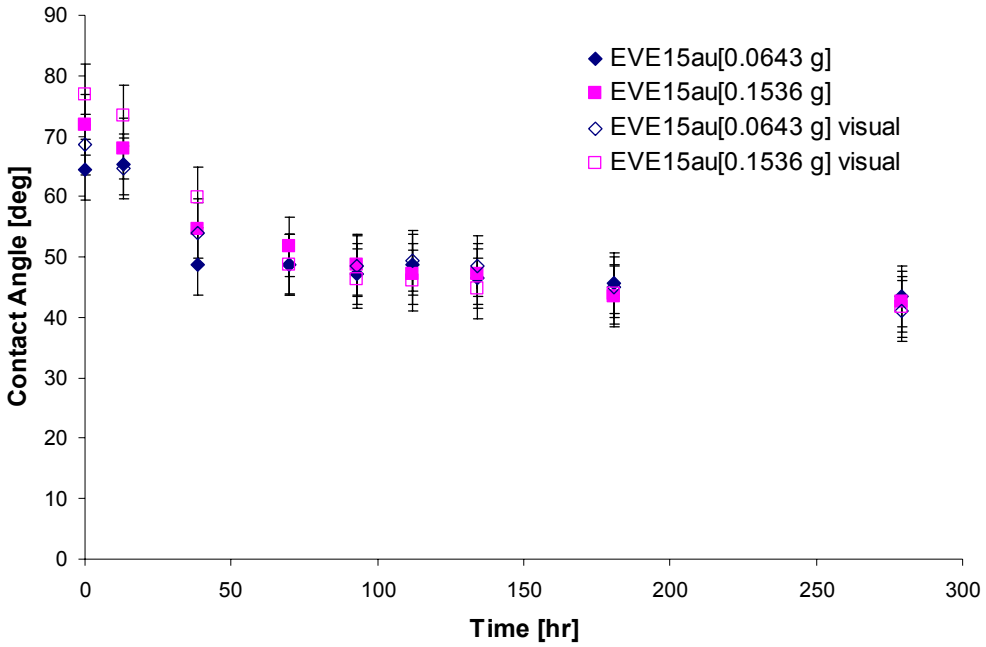

Figure 3.1.3: Contact angle versus time of EVE15ba brush coated sandstone

In this experiment two stones for each polymer were tested. The amount of polymer applied to the stones was roughly doubled from the first stone to the second. This was done to see if there is a significant difference in contact angle over time as a function of polymer thickness. Again due to the small amount of polymer only two stones were coated per polymer compound. For the EVE15au compound the contact angle stabilized at approximately 45 degrees over the course of the experiment. This was the case for both stones. The contact angle for the EVE15ba compound, however, stabilized at approximately 50 degrees for both stones. These measurements suggest that even though initial contact angles vary significantly with polymer thickness, over time the different coating thicknesses provide about the same protection. This decrease in

contact angle can be attributed to rearrangement of the polymer on the surface of the stone. It is also due to the harsh environment of the experiment. In real life the stones would not be subject to continual saturation in liquid water. However this is a relevant test because if the same protection can be achieved with lower polymer coverage, this is much more cost effective.

3.2 Brush Coating Protective Efficacy Measurements

In Figure 3.2.1 liquid water absorption measurements show the protective efficacy of the polymer coatings.

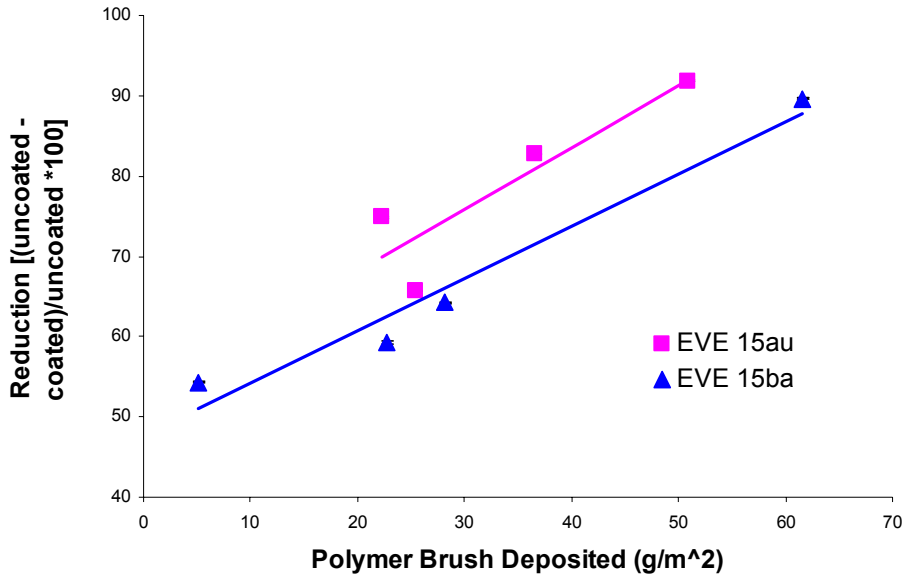

Figure 3.2.1: Protective efficacy of brush coated sandstone

The same set of stones tested in the contact angle experiments were used for the liquid water absorption experiments. The protective efficacy increases with polymer coverage. Again there is a slight decrease in the reduction of water absorption for EVE15au with increasing polymer thickness from the first to the second data point. This is again due to non uniformity in the stone samples. It can also be noted that the variation occurs in the same stone sample as that from the contact angle experiments. EVE15au coated stones displayed higher protective efficacies than EVE15ba coated stones for corresponding

polymer thickness. The highest protective efficacy obtained was approximately 90%, for 50 g/m^2 coverage of EVE15au. The stone coated with EVE (15)ba reached a maximum efficacy of approximately 87% at a coating of 65 g/m^2.

3.3 Brush Coating Water Vapor Diffusivity Measurements

The last performance evaluation of the brush coated stones was water vapor diffusivity. In figures 3.3.1 and 3.3.2 the water mass evaporation rates for EVE15ba and EVE15au coated stones are shown. Two stones for each polymer were tested. In addition, readings for aluminium substrate (for normalization) and uncoated stones are shown

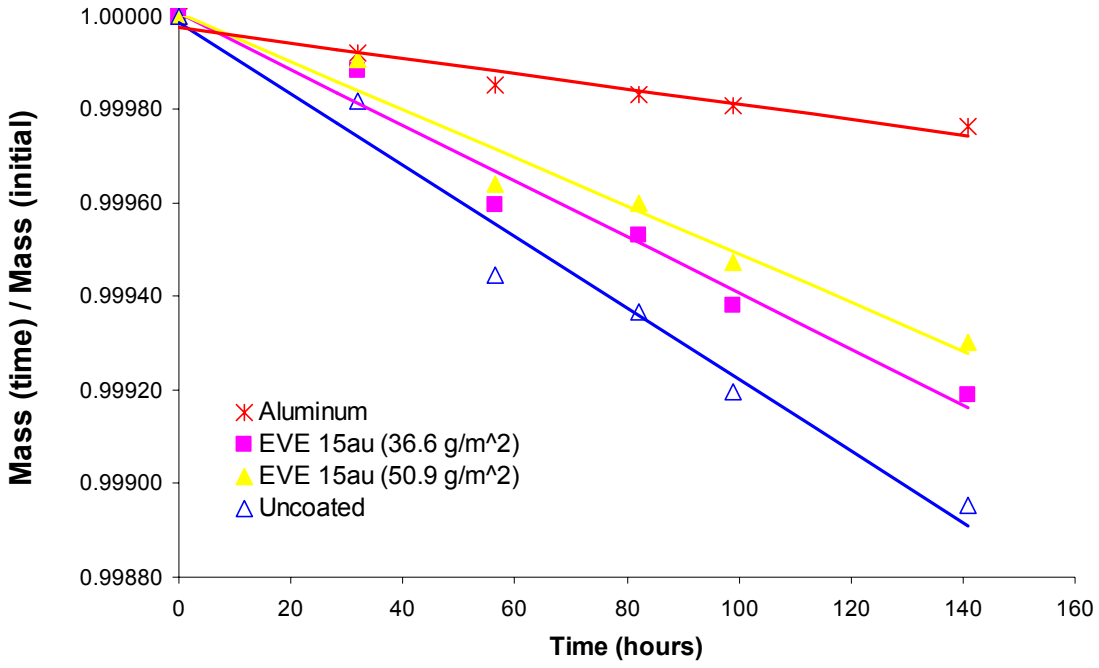

Figure 3.3.1: Water vapor transport of EVE15au brush coated sandstone

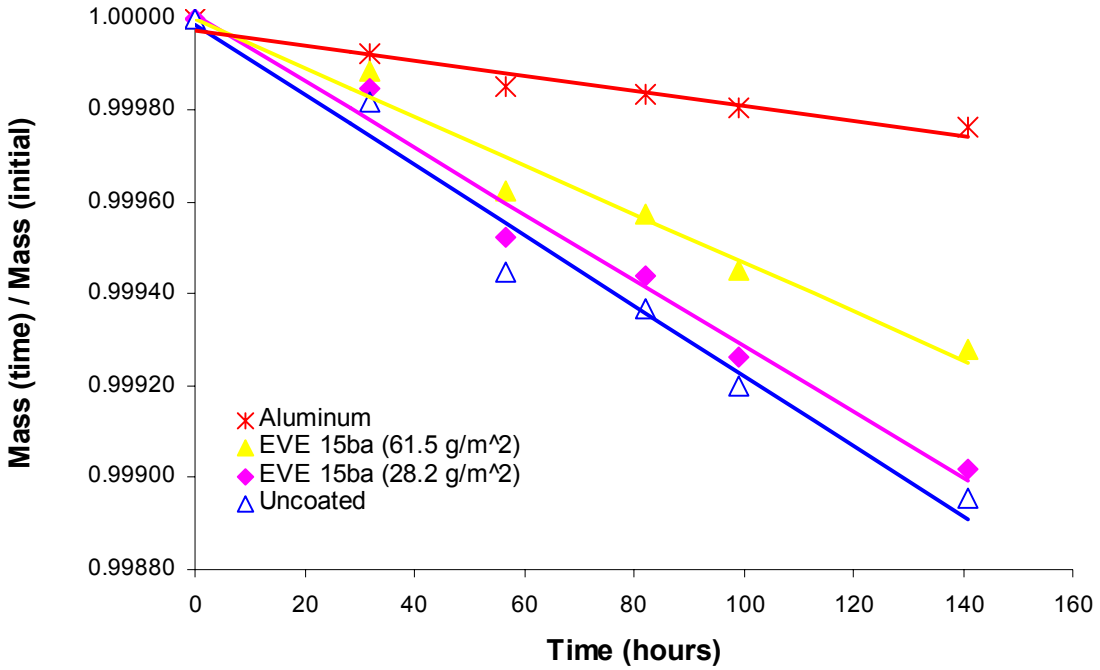

Figure 3.3.2: Water vapor transport of EVE15ba brush coated sandstone

Since measurements were not taken on the stones prior to coating, calculations of polymer penetration could not be calculated. The coated stones were then compared to that of a different uncoated stone. The important result seen in figures 3.3.1 and 3.3.2 is that the coating does not significantly reduce vapor transport through the stone. This is an important characteristic. If a protective coating is applied to a surface it must allow for vapor transport otherwise water can be trapped underneath the coating and actually accelerate the deterioration process of the stone.

3.4 Spray Coating

In previous work a similar polymer was characterized for RESS spray coating. That polymer (PFD) was of the same chemical structure of the UNC diamide, the only difference being the molecular weight of the two. The PFD is ~2500 M_w while the UNC diamide is ~3600 M_w.

Cloud point pressure versus temperature data of PFD/CO_2 and UNC diamide/CO_2 solution are shown below in figure 3.4.1. The measured composition of both solutions was roughly 2 wt%.

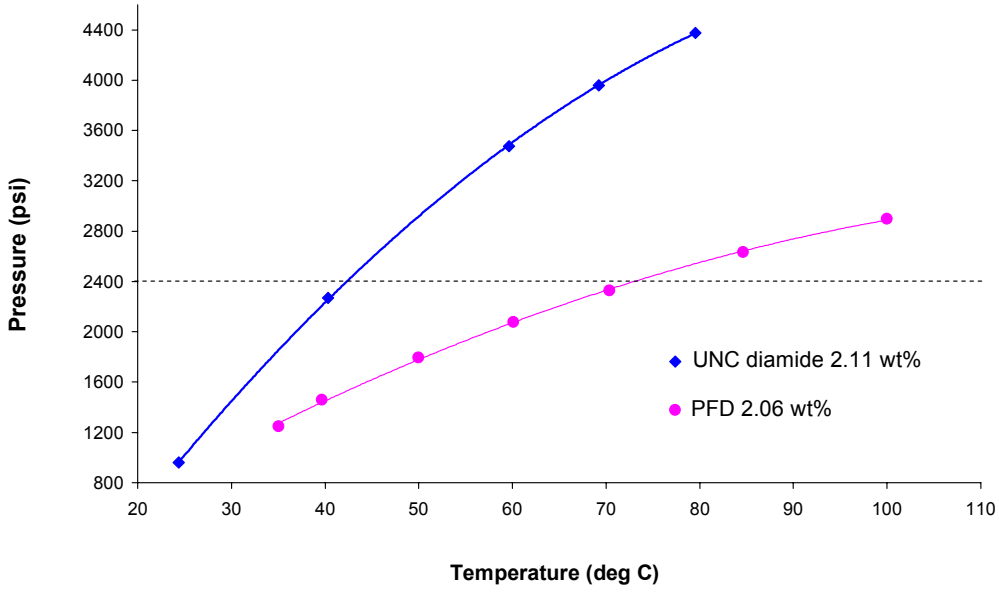

Figure 3.4.1: Measured cloud point curves

The dashed line represents the isobar (2400 psi) at which the majority of RESS experiments were conducted. The 2400 psi isobar is located under the cloud point curve

for the UNC diamide for temperatures above ~ 40 ºC. This has a significant effect on the droplet formation process, as described by figure 1.1. It can also be seen from the cloud point data, that the UNC diamide cloud point pressures are significantly higher than those of the PFD. Due to the large difference in the cloud point pressure, it proves difficult to compare the results of the current work with that of the preceding work. In order to compare the PFD and the UNC diamide, a plot of normalized process conditions was constructed and is shown in figure 3.4.2

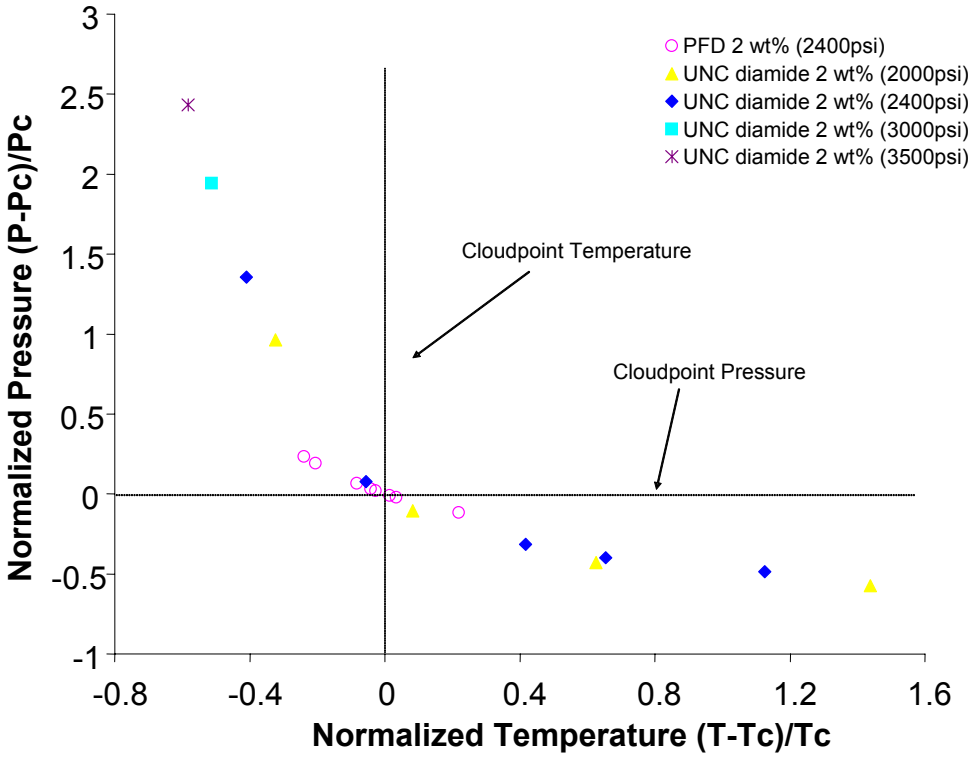

Figure 3.4.2: Normalized process conditions

The plot displays the process conditions of the transfer efficiency experiments conducted with the two polymers. Section 2.2.6 describes the transfer efficiency measurement

technique. The equilibrium temperature is defined as the cloud point temperature for a given pressure and concentration. A table of cloudpoint temperatures of process conditions for the transfer efficiency experiments is given below.

Table 3.4.1: Cloudpoint temperatures

UNC diamide 2wt%	
Pressure (psi)	Temperature, Tc (deg)
2000	36.9
2400	42.3
3000	51.3
3500	59.9
PFD 2 wt%	
2400	73.1

It is important to note that the PDF experiments were conducted over a narrower range of normalized conditions than the UNC diamide experiments.

Figure 3.4.3 displays the effect of pre expansion temperature and pressure on transfer efficiency. The solutions of polymer (UNC diamide and PFD)/CO_2 tested were at 2 wt% at varying pressures.

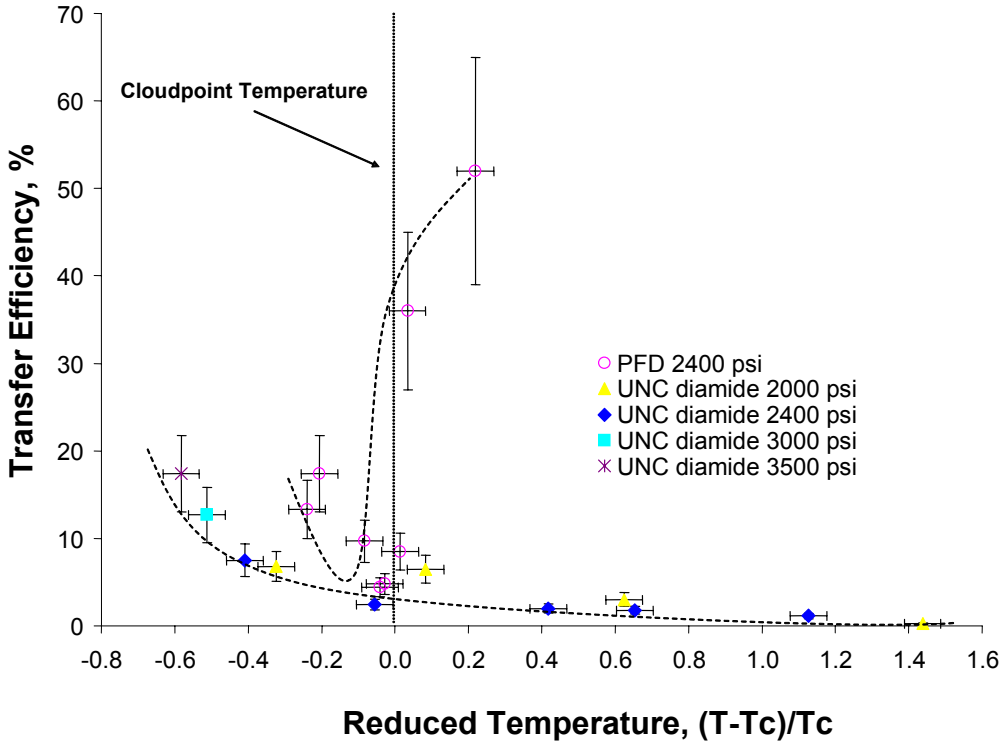

Figure 3.4.3: Transfer efficiency of the PFD and UNC diamide

The vertical line in figure 3.4.3 represents the cloudpoint temperature for the solutions. Below the equilibrium temperature droplets are formed by nucleation due to expansion through the nozzle. The PFD/CO_2 solution produced higher transfer efficiencies compared to the UNC diamide at similar temperature and pressure conditions. When the pre-expansion pressure was raised for the UNC diamide it resulted in higher transfer efficiencies. However during the experiments at 3000 and 3500 psi ice formed on the surface of the stone. This growing ice deposit possibly allowed a greater amount of polymer to collect. The ice may have trapped polymer that would have been swept off

the surface if it were not present. A series of photographs that show the process of polymer application at 3500 psi and 25 degrees C is shown in figure 3.4.4.

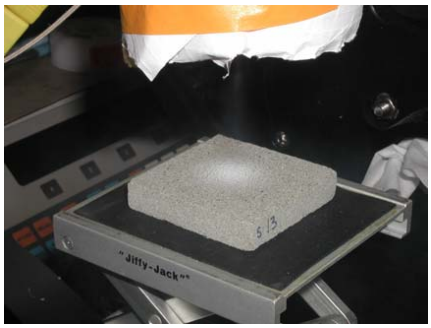

Ice begins to form on surface

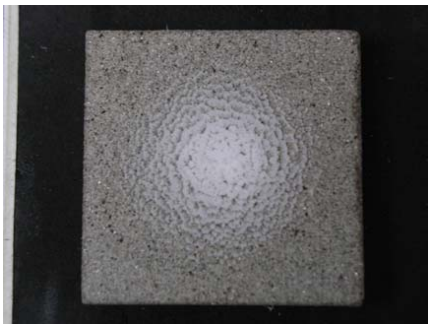

Ice continues to grow

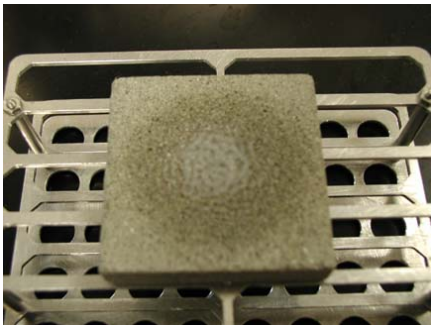

5 Min after: ice melting leaving

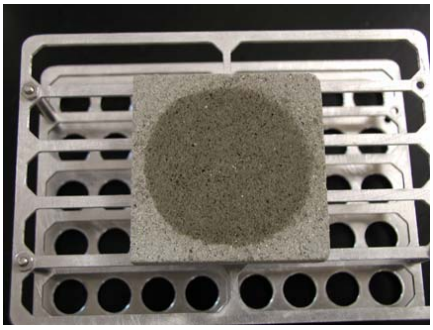

Overnight: the polymer spreads out

Figure 3.4.4: Spray coating at 3500 psi and 25 degrees C

To the right of the vertical line in figure 3.4.3 represents the point at which the solutions cross the cloud point curve. At this point, assuming thermodynamic equilibrium, the solution precipitates prior to entering the nozzle. In the case of the PFD, tendrils of polymer are formed at the nozzle exit. This results in a high transfer efficiency, however the spray product is not desirable. The polymer tendrils do not adhere to the stone surface rendering the coating ineffective. The UNC diamide did not exhibit this behavior. From this data it can be seen that as temperature increases transfer

efficiency continues to decrease. Even though the temperature was well above the equilibrium temperature, there was no clogging of the nozzle or lines. The observed spray at elevated temperatures was almost completely void of polymer. It is conjectured that the spray conditions were so far above the solubility limit that the polymer precipitated to the bottom of the ISCO pump only to be deposited along the lines of the system and therefore not reaching the nozzle. It was observed during cleaning of the spray apparatus system that there was a significant amount of polymer ejected from the system at these conditions. There are other factors that effect transfer efficiency. In this study the stones were located 5 cm from the nozzle exit. It is possible that this is not the optimum distance for coating. If the stone is too close to the nozzle particles may bounce off of the stone. Also, particles may be swept off the surface due to the close proximity of the high pressure flow exiting the nozzle. Conversely, if the stone is positioned too far downstream of the nozzle the flow pattern will extend outside of the stone surface. Polymer droplets will pass by the stone without ever contacting the surface. In addition to distance from the nozzle, spray pattern and spray angle are also important aspects of coating. These issues were not dealt with in this investigation.

The effect of process conditions on measured UNC diamide 2 wt% droplet size distributions can be seen in figure 3.4.5. These plots represent the droplet diameter as a function of volume frequency.

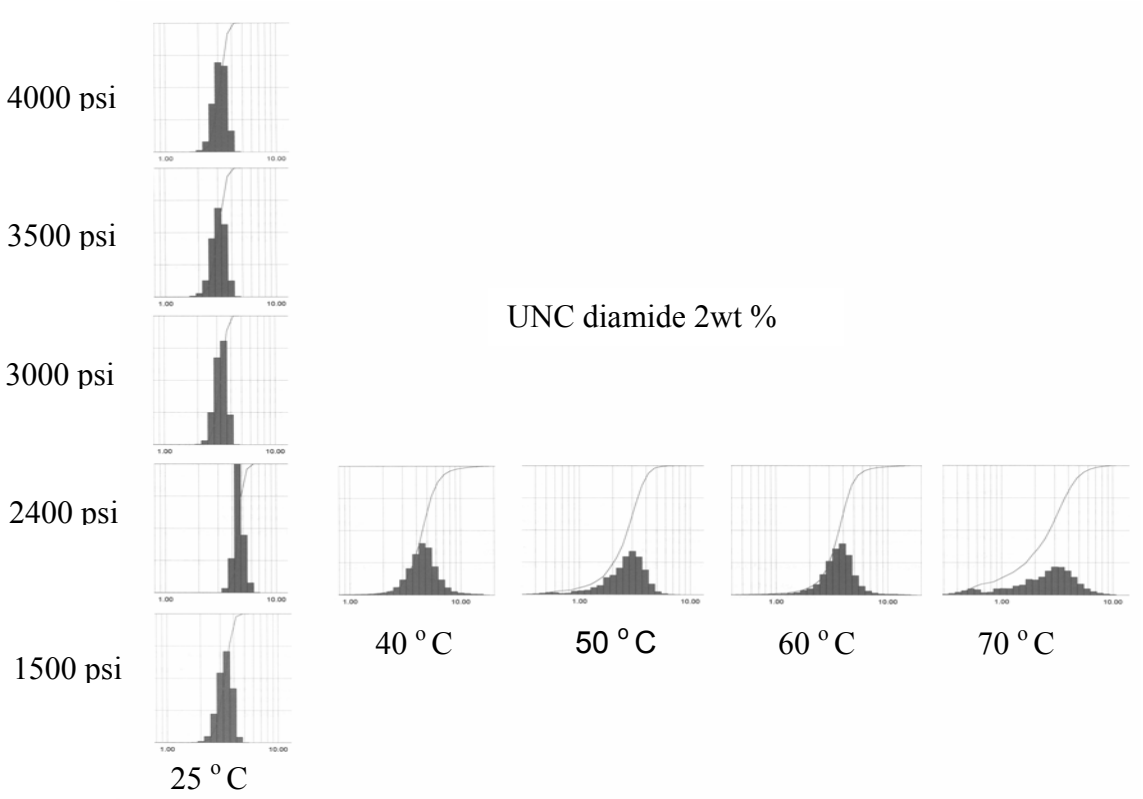

Figure 3.4.5: Effect of temperature and pressure on particle size distribution of UNC-diamide

As seen in previous experimentation using PFD (refer to figure 1.4) increasing temperature leads to wider droplet size distributions. This is also seen with the UNC-diamide as indicated in figure 3.4.5. Increasing pressure had a slight effect on particle size distribution. An increase in pressure from 1500 to 2400 psi produced a narrower particle size distribution, while an increase in pressure from 2400 to 3000 psi produced a wider particle size distribution. Further increases in pressure had a negligible effect on the particle size distribution. The effect of temperature on 50% cumulative volume

(Dv(50)) and Sauter mean diameter (D[3][2])) of 2wt% UNC-diamide at 2400 psi can be seen in figures 3.4.6 and 3.4.7

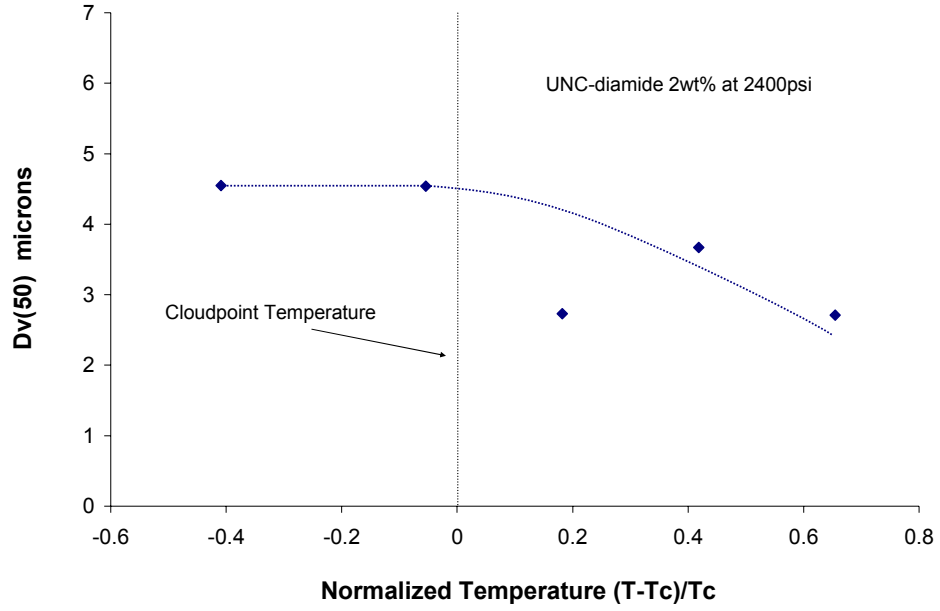

Figure 3.4.6: Effect of temperature on Dv(50) of 2wt% UNC-diamide

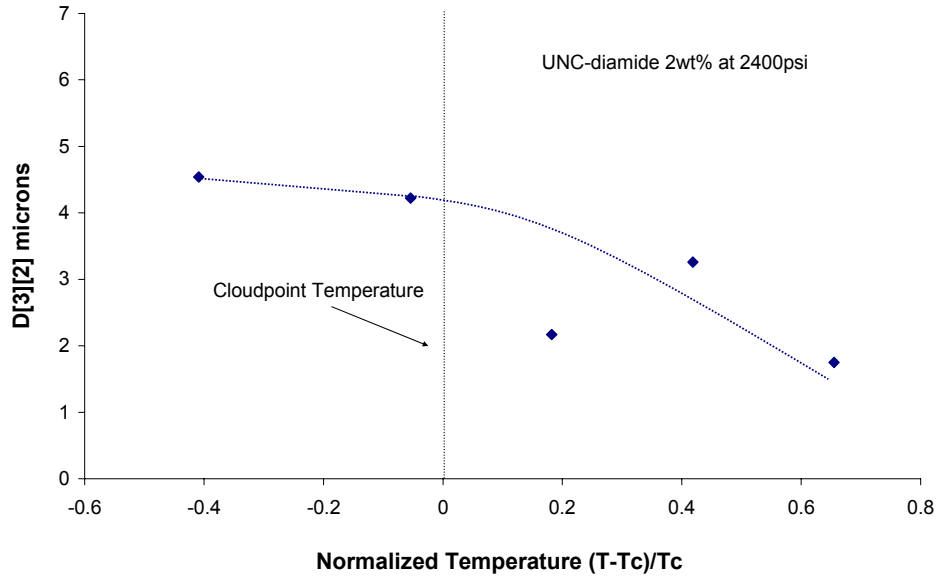

Figure 3.4.7: Effect of temperature on D[3][2] of 2wt% UNC-diamide

The readings of Dv(50) and D[3][2] were recorded simultaneously at each temperature. As seen in previous work, variation in temperature above the cloupoint curve does not have a significant effect on Dv(50) particle size. It remained constant at a value of 4.5 microns. The size of the particles are approximately 1 micron larger than the results seen with the PFD study. There was a slight decrease in Sauter mean diameter as temperature increased below the cloudpoint curve. This is also consistent with previous work. [29] Below the cloudpoint curve, increasing temperature reduced the size of Dv(50) and Sauter mean diameter.

The effect of pressure on 50% cumulative volume (Dv(50)) and Sauter mean diameter (D[3][2]) of 2wt% UNC-diamide at 25 ºC can be seen in figures 3.4.8 and 3.4.9.

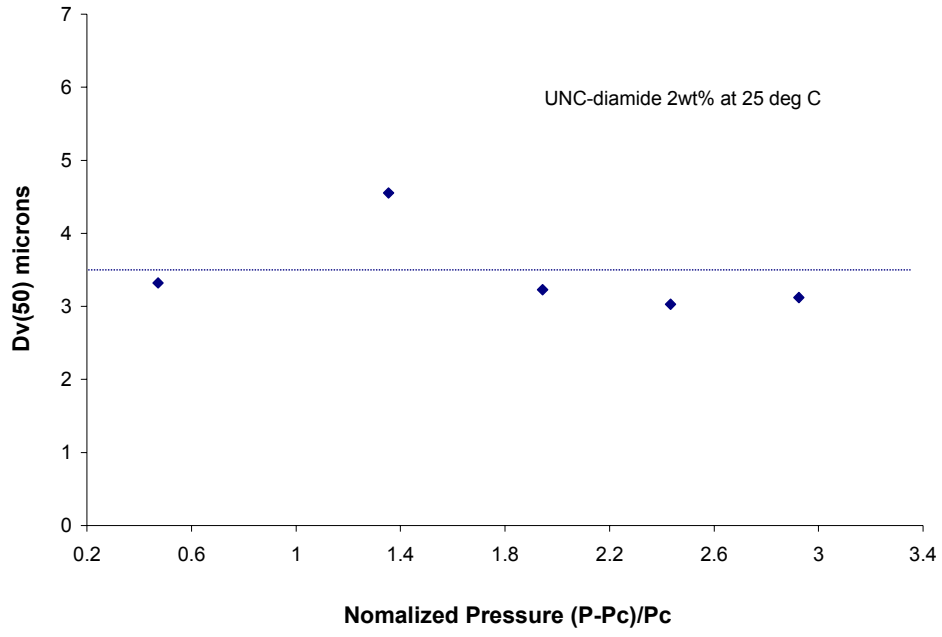

Figure 3.4.8: Effect of pressure on Dv(50) of 2wt% UNC-diamide

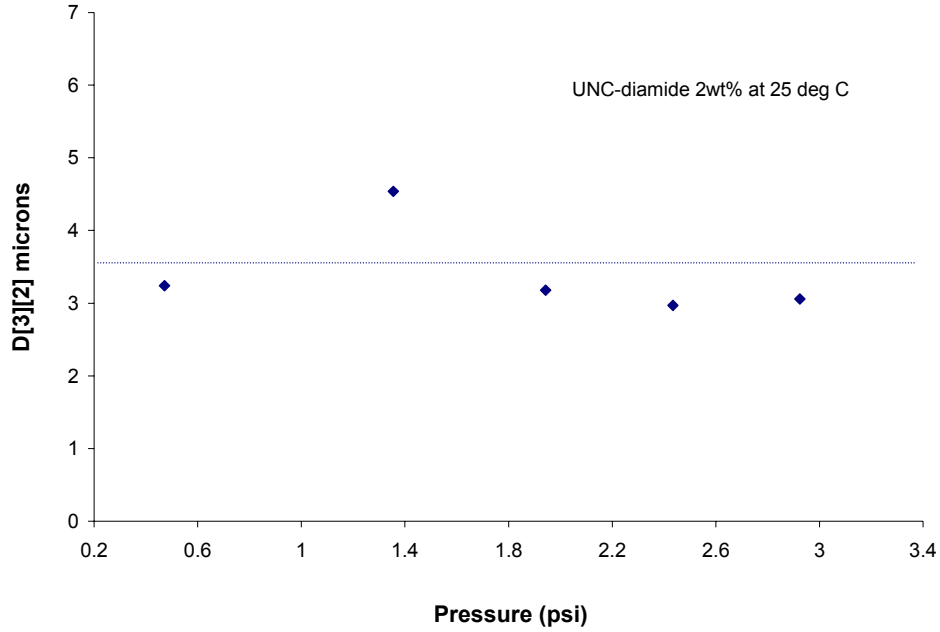

Figure 3.4.9: Effect of pressure on D[3][2] of 2wt% UNC-diamide

The readings of Dv(50) and D[3][2] were recorded simultaneously at each pressure. Increasing pressure had negligible effect on the particle size of both the Dv(50) and D[3][2] measurements, with the exception of normalized pressure of 1.35. The particles sizes ranged between 3 to 3.2 microns. This particle size is consistent with previous study of PFD. The normalized pressure of 1.35, which corresponds to 2400 psi at 25 ºC, produced a particle size of 4.5. Recall from figure 3.4.5 that this condition also produced a slightly narrower particle size distribution that other RESS process conditions.

3.5 RESS Contact Angle Measurements

Figure 3.5.1 shows the measured contact angles of liquid water for the spray coated sandstone. The two methods of measurement, height calculations and visual inspection, are displayed on the graph versus amount of UNC-diamide polymer coating.

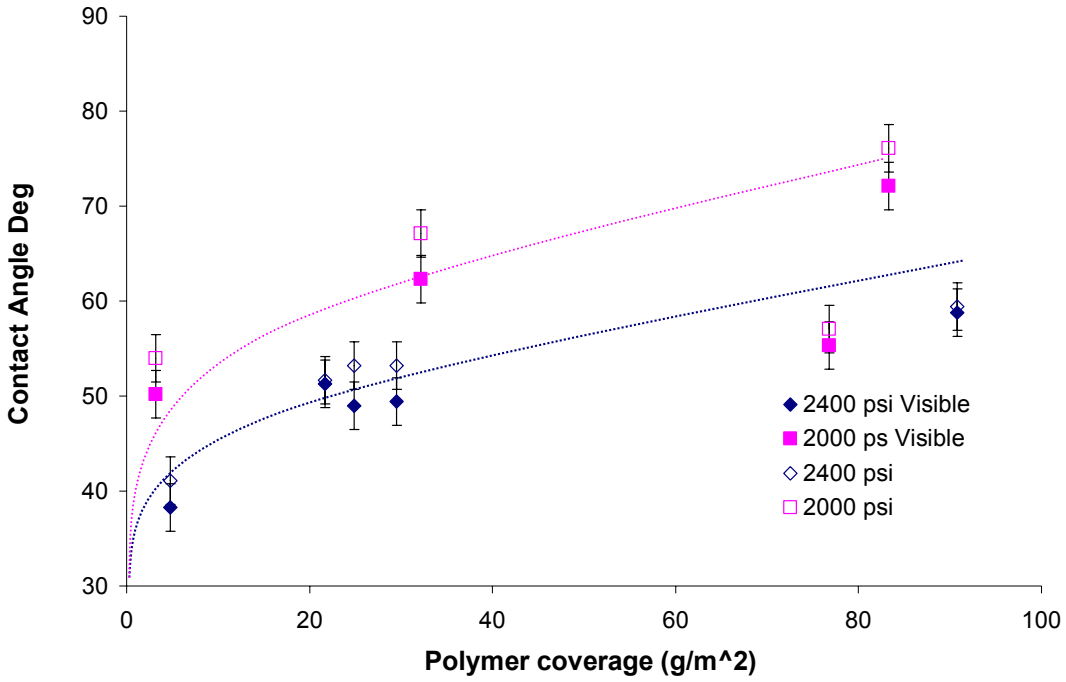

Figure 3.5.1: Contact angles of UNC-diamide spray coated sandstone

It can be seen that the two methods give contact angles to within five degrees of each other. As expected the contact angles increase with increase in polymer thickness. There is one point that did not follow the trend. The contact angle for the case of ~76 g/m^2 at 2000 psi was lower than expected. As observed with the brush coated experiments this can be contributed to non-uniformity of the sandstone specimens. None of the coatings

produced a non-wetting surface. The highest contact angle produced by spray coating was approximately 75 degrees, for 85 g/m^2 at 2000 psi. It can also be observed that the coating at 2000 psi produced a higher contact angle than the 2400 psi coating for similar polymer thickness. A polymer coverage value was not reached where the contact angles reached a maximum. The RESS process used to coat the stones is a batch process. For the given process the maximum amount of polymer was delivered to the surface. To increase the coverage a second spray coating process would be required. This study focused only on single spray coatings.

As before with the brush coated sandstone, the effect of continual water exposure was examined for spray coated stones. This experiment was carried out on the same set of spray coated stones used in the initial contact angle, water absorption and water vapor diffusivity experiments. There was expected to be some deterioration of the polymer coating's performance with time. Figures 3.5.2 and 3.5.3 display the results of the exposure experiment. For ease of viewing only the calculated contact angle measurements are displayed. The value of all the contact angles are given in tables 3.5.1 and 3.5.2.

Table 3.5.1 Calculated and visual contact angles for 2400 psi RESS coatings

Time	90.80 g/m^2		29.52 g/m^2		24.84 g/m^2		21.68 g/m^2		4.80 g/m^2	
(hrs)	Height	Visual	Height	Visual	Height	Visual	Height	Visual	Height	Visual
0	59.17	57.10	49.57	46.00	50.17	46.10	48.67	49.00	41.26	39.30
24	54.72	56.50	47.70	48.90	49.47	51.40	51.71	52.30	41.24	42.90
50	53.19	51.80	48.67	46.90	47.17	46.30	50.17	49.20	41.10	39.30
72	54.72	52.20	48.36	46.50	50.17	49.60	51.68	50.00	37.94	35.90
94	47.17	45.90	53.19	51.70	45.67	43.50	47.17	48.60	41.10	38.90
170	42.64	44.00	47.17	45.20	47.30	44.90	42.64	42.00	41.14	38.90

Table 3.5.2 Calculated and visual contact angles for 2000 psi RESS coatings

Time	83.28 g/m^2		76.80 g/m^2		32.16 g/m^2		3.20 g/m^2	
(hrs)	Height	Visual	Height	Visual	Height	Visual	Height	Visual
0	70.26	68.30	61.05	60.90	59.43	56.00	51.27	48.40
24	66.18	68.20	61.73	59.90	57.53	57.10	50.04	49.30
50	69.89	67.70	61.28	62.30	56.46	57.70	45.67	46.70
72	59.43	57.40	61.05	58.00	57.83	55.80	42.57	39.10
94	54.72	52.70	56.27	54.80	48.67	46.20	45.67	45.20
170	47.17	48.70	47.17	45.20	46.30	45.20	42.53	39.90

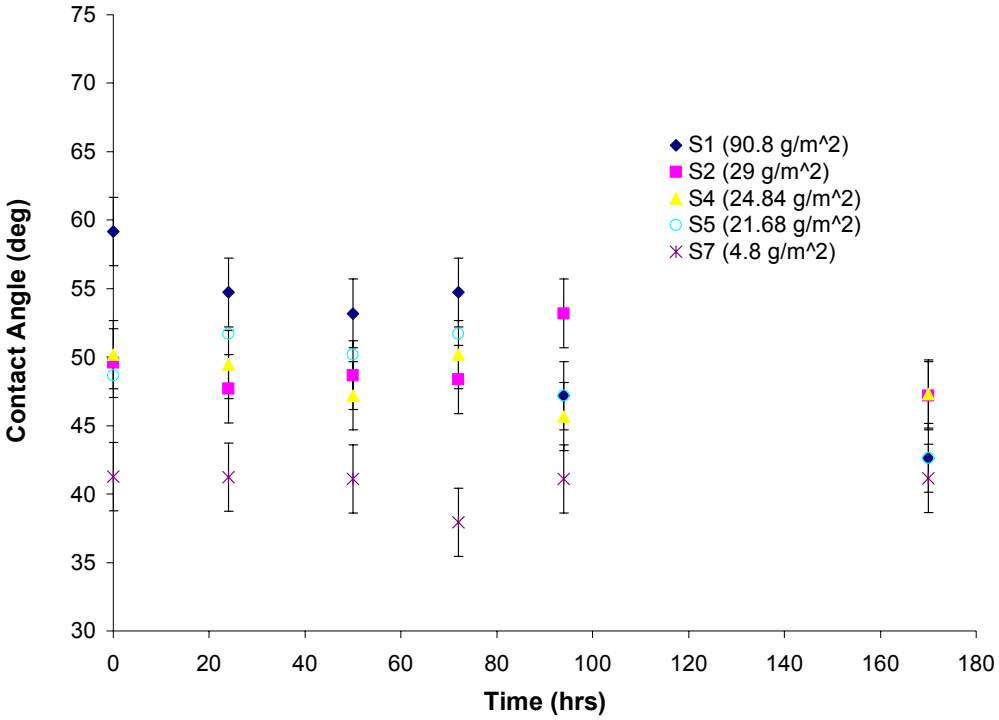

Figure 3.5.2: Contact angle versus time of UNC diamide at 2400 psi spray coated sandstone

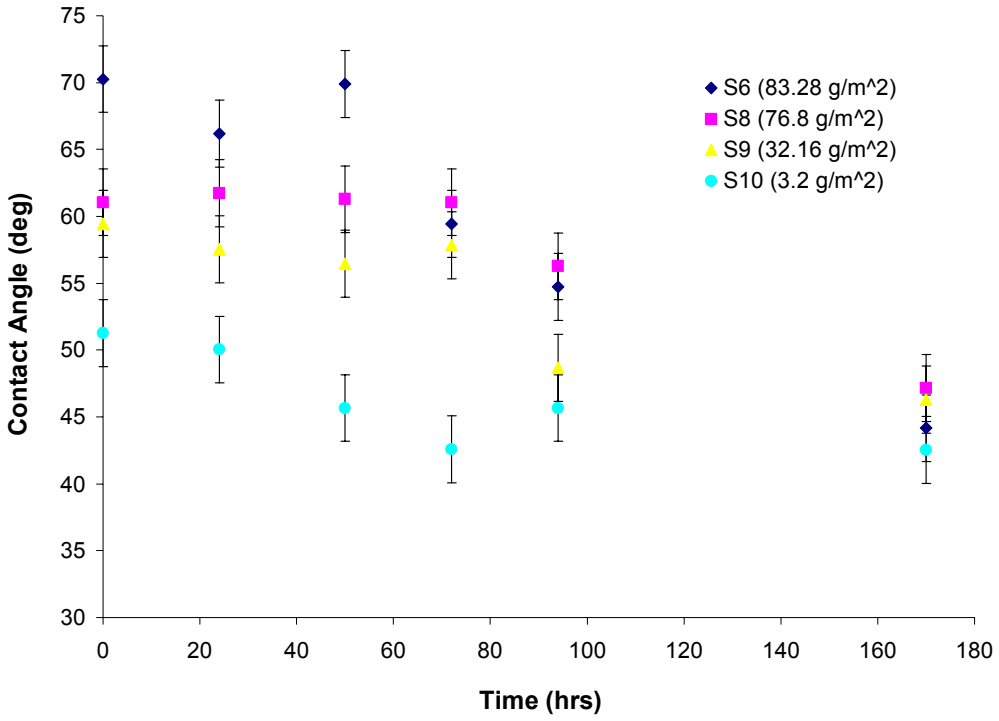

Figure 3.5.3: Contact angle versus time of UNC diamide at 2000 psi spray coated sandstone

The first point to note from these results is that the time 0 hr contact angle readings are approximately the same as those recorded in initial contact angle readings. The readings are in agreement to within the +/- 2.5 degrees experimental error. This suggests that the experiments (contact angle, water absorption and diffusivity) performed on the stones did not reduce the coatings protective performance. The initial contact angles vary significantly depending on polymer coverage. These values are displayed for comparison in table 3.5.3

Table 3.5.3: Height calculated contact angles of spray coated stones

	Polymer coating (g/m^2)	Initial contact angle (degrees)	Contact angle (t = 0 hrs) (degrees)
2400 psi	90.80	58.8	59.2
	29.52	49.4	49.5
	24.84	49.0	50.2
	21.68	51.3	48.7
	4.80	38.3	41.3
2000 psi	83.28	72.1	70.3
	76.80	55.3	61.1
	32.16	62.3	59.4
	3.20	50.2	51.3

Over the course of the experiment the contact angles decreased to approximately 45 degrees for both the 2000 and 2400 psi coatings. This is essentially the same result seen in the brush coating experiments.

3.6 RESS Protective Efficacy Measurements

Figure 3.6.1 displays the protective efficacy of the spray coating.

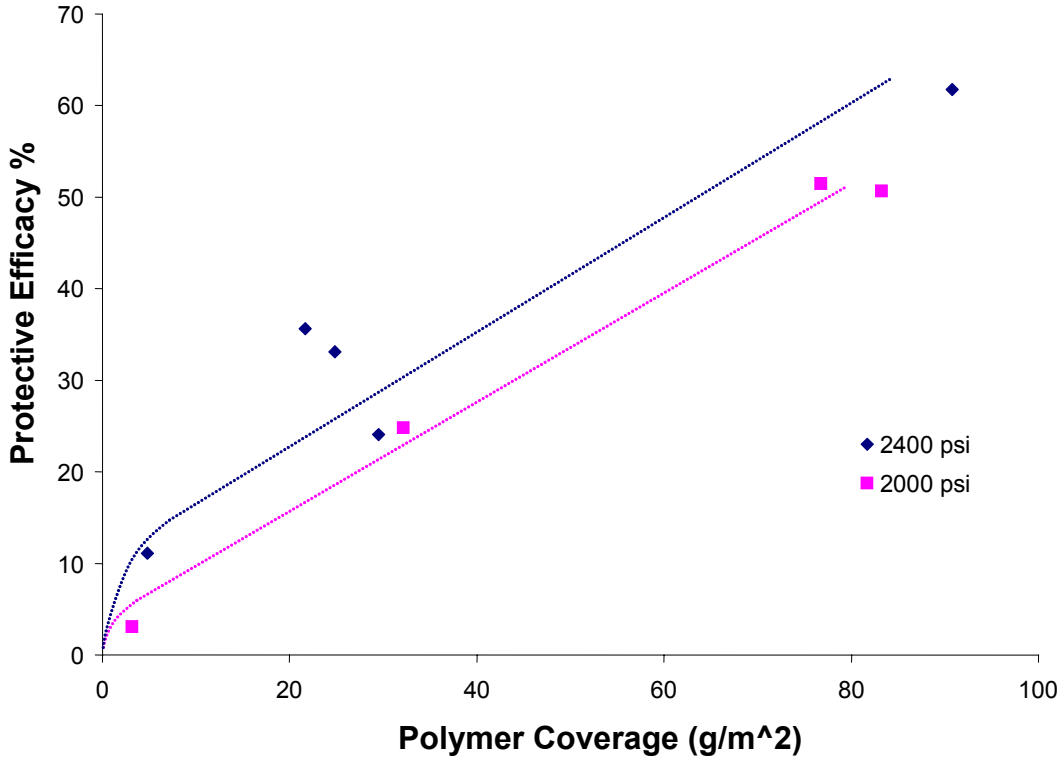

Figure 3.6.1: Protective efficacy of UNC-diamide spray coated sandstone

The same set of stones tested in the contact angle experiment was used for the liquid water absorption study. As expected, the protective efficiency increases with polymer coverage. There are two points that are slightly outside of the trend for the 2400 psi case. This again could be due to non uniformity in the stone samples. The difference in pre-expansion pressures did not have a dramatic effect on protective efficacy.

3.7 RESS Water Vapor Diffusivity Measurements

In figures 3.7.1 and 3.7.2 the water mass evaporation rates for spray coated stones are presented.

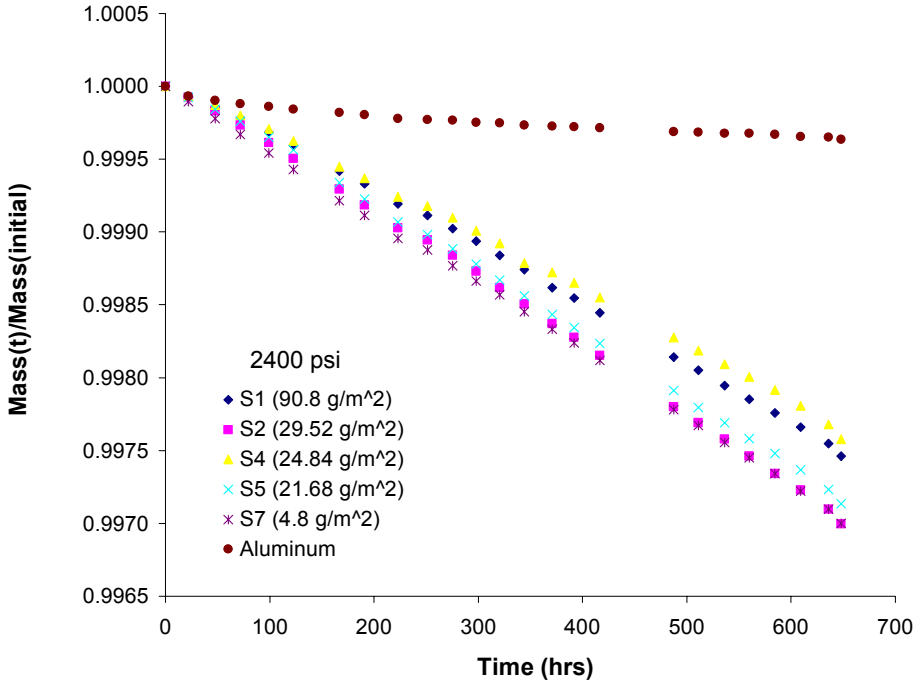

Figure 3.7.1: Water vapor transport through UNC-diamide spray coated sandstone

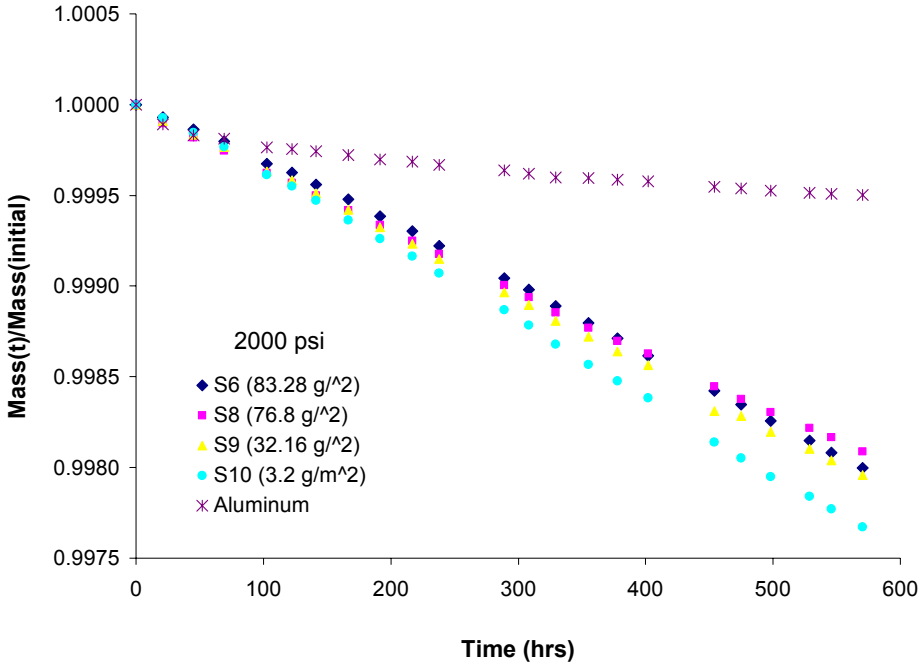

Figure 3.7.2: Water vapor transport through UNC-diamide spray coated sandstone

As expected the water vapor transport is a linear function of time. A perfect seal of the canisters can not be obtained. This can be seen by the water vapor loss of the aluminum block. This is due to bypass of the seal of the canister. As mentioned in section 2.5 the water vapor loss of the aluminum block is subtracted from that of the other containers. Water vapor transport rates were obtained for the uncoated stones used in the spray coating experiments. Theses values could then be used to analyze the results from spray coating. Figure 3.7.3 displays the percent reduction of water vapor transport through the coated stones.

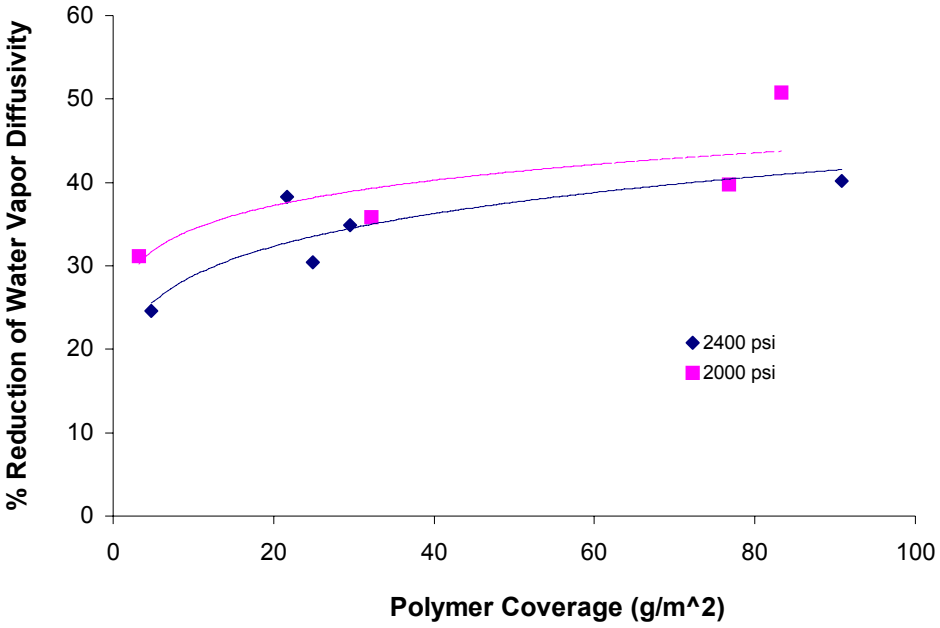

Figure 3.7.3: Water vapor diffusivity reduction of spray coated sandstone

The percent reduction is calculated as:

$$\%\,\text{Reduction} = {(\text{massflux uncoated} - \text{coated})}/{\text{uncoated}} * 100 \qquad (3.7.1)$$

As expected, as polymer coverage increases the percent reduction increases. The increase in water vapor diffusivity however is not dramatic. Over the span of polymer coverage the percent reduction ranges from ~25% to ~40%. This shows that the polymer coatings do not significantly prevent water vapor transport through the stone. There was one high point that was outside the trends of both plots. This can as well be attributed to non uniformity of the stone samples or non-uniformity of the coating applied.

Figure 3.7.4 displays the penetration depth of the polymer for the spray coated stones.

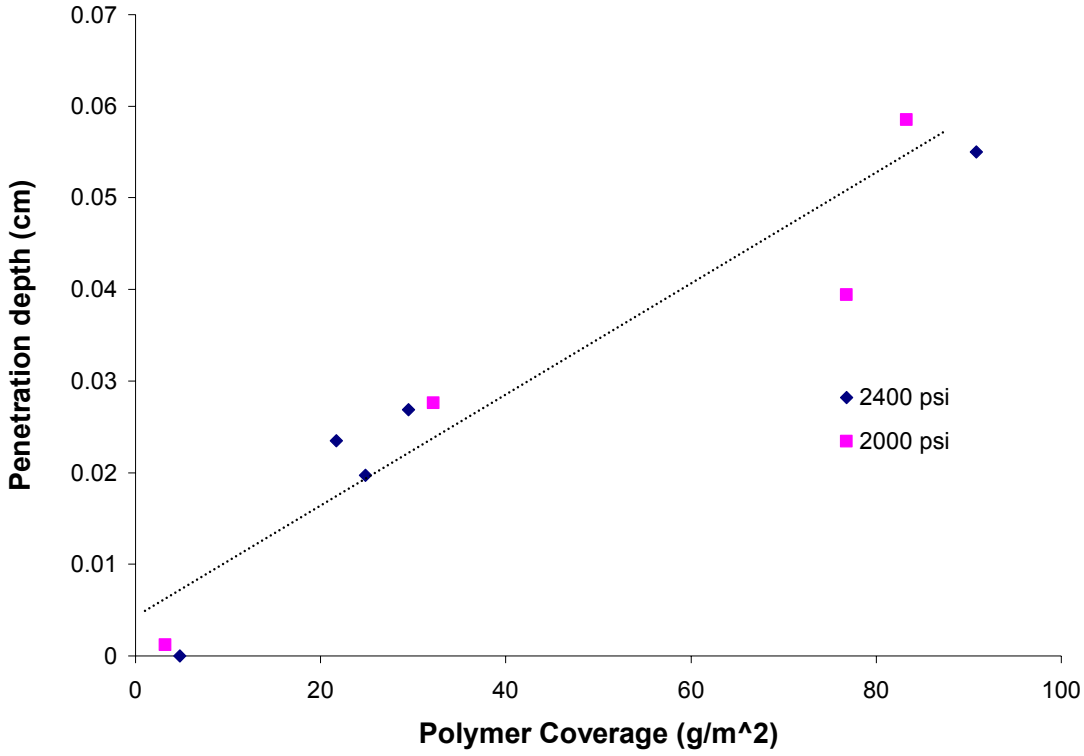

Figure 3.7.4: Polymer penetration depth of UNC-diamide spray coated stones

The penetration depth increases with polymer coverage. This is to be expected as there is more polymeric material to penetrate the stone at higher coverage. There was no significant difference between the 2000 psi and 2400 psi cases. This is to be expected as the polymer is a liquid at room temperature and penetration is most effected by the amount of polymer deposited and its viscosity.

Figure 3.7.5 shows the reduction in porosity of the coated layer of the spray coated stones.

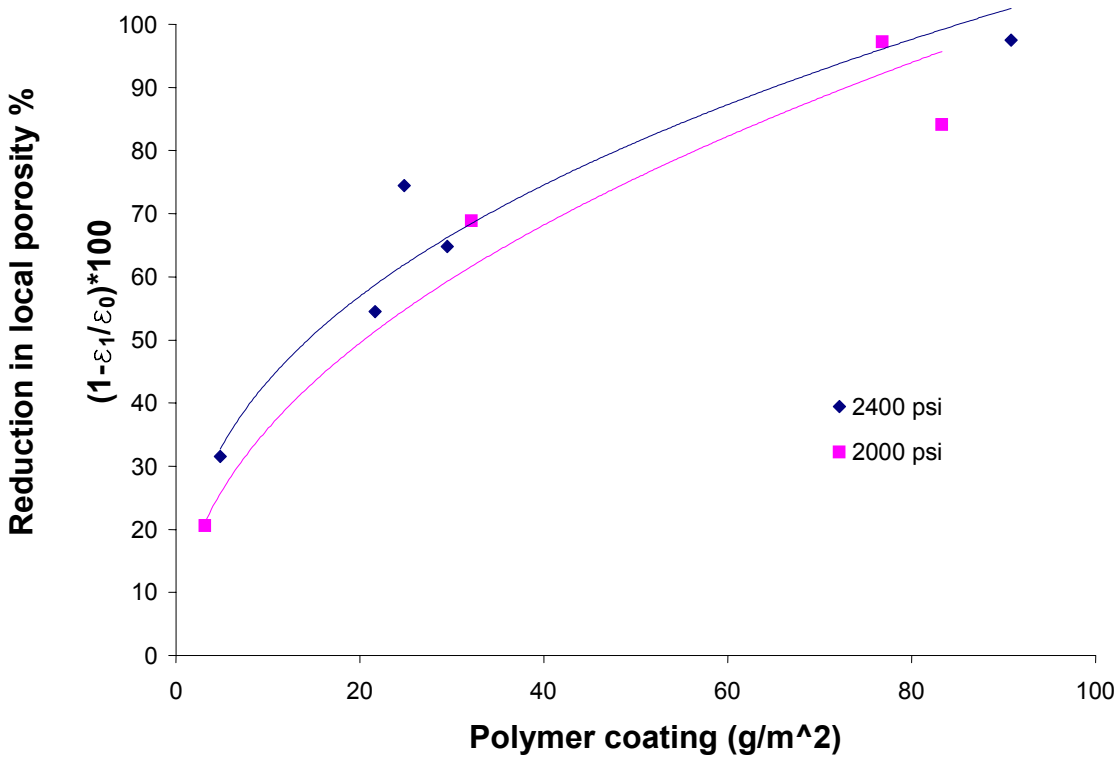

Figure 3.7.5: Water vapor transport through spray coated sandstone

The results follow the expected trend. As the polymer thickness increases the reduction in porosity increases rapidly. Previous work with perflouropolyether diamides has shown this trend as well, however, as the polymer coating continued to increase the reduction of porosity began to decrease to a value of approximately 80 %. [21]

4. Conclusions

Two perflouropolyether coating compounds developed by Bunyard at UNC-Ch (EVE15au and EVE15ba) have been experimentally evaluated on sandstone. These polymers were evaluated for water droplet wetting, reduction of liquid water absorption and water vapor diffusivity. As the polymer coating thickness increased, contact angles of water droplets approached non-wetting criteria. The highest contact angle achieved, ~ 75 degrees, was for 50 g/m^2 coating of EVE15au. The contact angles of coated sandstones were then examined for the effect of prolonged submersion in liquid water. It was found that as submersion time increased the contact angle decreased to a value ~ 45 to 50 degrees regardless of polymer coating type. Increasing polymer coating thickness also resulted in an increase protective efficacy. The highest protective efficacy obtained was approximately 90%, for 50 g/m^2 coverage of EVE15au. The increase of polymer coating did not significantly block water vapor transport through the sandstones.

The relationship between droplet and spray characteristics for RESS process conditions were evaluated for UNC diamide. As temperature increased transfer efficiency decreased and a wider droplet distribution was seen. Increases in pressure resulted in higher transfer efficiency yet had only a slight effect on droplet size distribution. An increase in pressure from 1500 to 2400 psi produced a more narrow size distribution, while an increase in pressure from 2400 to 3000 psi produced a wider size distribution. Further increases in pressure had a negligible effect on the particle size distribution.

In addition to droplet and spray characteristics the evaluation of the coating effectiveness on sandstone at different RESS process conditions was studied. These experiments included water droplet wetting, reduction of liquid water absorption and water vapor diffusivity. Increases in polymer coating thickness led to higher contact angles and increases in the reduction of liquid water absorption and reduction of water vapor transport. The highest contact angle produced by spray coating was approximately 75 degrees, for 85 g/m^2 at RESS conditions of 2000 psi and 25 ºC. The stones coated at 2000 psi displayed slightly higher contact angles than the stones coated at 2400 psi over the range of polymer coatings. The effect of extended submersion in liquid water was also observed. As the time of submersion increased the contact angles of the coated stones decreased to approximately a value of 45 to 50 degrees regardless of the polymer coating.

The highest protective efficacy obtained was approximately 60%, for 90 g/m^2 at RESS conditions of 2400 psi and 25 ºC. The difference between the coatings sprayed at RESS conditions of 2400 and 2000 psi was negligible. The largest reduction of water vapor transport was approximately 50% for 85 g/m^2 at 2000 psi and 25 ºC. The UNC diamide spray coating did not significantly reduce the water vapor transport over that of an uncoated stone.

The spray coatings penetration depth increased with polymer coverage. The maximum depth of 0.055 cm was achieved for 85 g/m^2 at RESS conditions of 2000 psi and 25 ºC. The reduction in porosity of the coated layer was high. A maximum of ~95% was reached at two conditions, 77 g/m^2 at 2000 psi and 25 ºC and for 90 g/m^2 at 2400 psi and 25 ºC.

5. References

1. Castelvetro, V., et al., *Adapting the Properties of New Fluorinated Acrylic Polymers to Suit the Conservation of Ancient Monuments.* Surface Coatings International, 1998(11): p. 551-556.

2. Piacenti, F., et al. *New Developments in Perfluorinated Protective Agents for Stone*. in *International RILEM/UNESCO Congress on Conservation of Stones and Other Materials*. 1993. Paris, France: E&FN Spon, London.

3. Ohsaka, Y., *Perfluoropolyethers.* Petrotech, 1985. **8**(9): p. 840.

4. Piacenti, F. and M. Camaiti, *Synthesis and Characterization of Fluorinated Polyetheric Amides.* J. of Fluorine Chem., 1994. **68**: p. 227-235.

5. Matteoli, U., et al. *Perfluoropolyether Isobutylamide and Isobutylester. Performance in the Protection of Stones*. in *VI th International Congress on Deterioration and Conservation of Stone*. 1988. Torun, Poland: Nicholas Copernicus University - Press Department, Torun, Poland.

6. Sianesi, D., et al., *Perfluoropolyethers: their Physical Properties and Behavior at High and Low Temperatures.* Wear, 1971. **18**: p. 85-100.

7. Piacenti, F., *Chemistry for the Conservation of the Cultural Heritage.* Sci. Total Environ., 1994. **143**: p. 113-120.

8. DeSimone, J.M., Z. Guan, and C.S. Elsbernd, *Synthesis of Fluoropolymers in Supercritical Carbon Dioxide.* Science, 1992. **257**: p. 945-947.

9. Brennecke, J.F. and C.A. Eckert, *Phase Equilibria for Supercritical Fluid Process Design.* AIChE J., 1989. **35**(9): p. 1409-1427.

10. Lele, A.K. and A.D. Shine, *Effect of RESS Dynamics on Polymer Morphology.* Ind. Eng. Chem. Res., 1994. **33**(1994): p. 1476-1485.

11. Matson, D.W., R.C. Petersen, and R.D. Smith, *Formation of silica powders from the rapid expansion of supercritical solutions.* Advance in Ceramic Material, 1986. **1**(3): p. 242-246.

12. Mohamed, S.R., P.G. Debenedetti, and R.K. Prud'homme, *Effects of Process Conditions on Crystals Obtained from Supercritical Mixtures.* AIChE J., 1989. **35**(29): p. 325-328.

13. Tom, J.W. and P.G. Debenedetti, *Particle Formation With Supercritical Fluids - A Review*. J. Aerosol Science, 1991. **22**(5): p. 555-584.

14. Mawson, S., et al., *Formation of Poly(1,1,2,2-tetrahydroperfluorodecyl acrylate) Submicron Fibers and Particles from Supercritical Carbon Dioxide Solutions.* Macromolecules, 1995. **28**: p. 3182-3191.

15. Chang, C.J. and A.D. Randolf, *Precipitation of Microsize Organic Particles from Supercritical Fluids.* AIChE Journal, 1989. **35**(11): p. 1876-1882.

16. Debenedetti, P.G., *Homogeneous Nucleation in Supercritical Fluids.* AIChE, 1990. **36**(9): p. 1289-1298.

17. Debenedetti, P.G., et al., *Rapid Expansion of Supercritical Solutions (RESS): Fundamentals and Applications.* Fluid Phase Equilibria, 1993. **82**: p. 311-321.

18. Ksibi, H., et al. *Hydrodynamic and Thermodynamic Profiles of a Supercritical Fluid Expansion Applied to the RESS Process*. in *3 rd International Symposium on Supercritical Fluids*. 1994. Strasbourg, France.

19. Kim, J.-H., T.E. Paxton, and D.L. Tomasko, *Microencapsulation of Naxopren Using Rapid Expansion of Supercritical Solutions.* Biotech. Prog., 1996. **12**: p. 650-661.

20. Domingo, C., E. Berends, and G.M. Van Rosmalen, *Precipitation of Ultrafine Organic Crystals from the Rapid Expansion of Supercritical Solutions over a Capillary and a Frit Nozzle.* Journal of Supercritical Fluids, 1997. **10**: p. 35-55.

21. Henon, F.E., *Environmentally Benign Polymer Coating Process for the Protection of Monumental Civil Infrastructures*, in *Department of Chemical Engineering*. 1999, North Carolina State University: Raleigh.

22. Liu, G.T. and K. Nagahama, *Solubility and RESS Experiments of Solid Solution in Supercritical Carbon Dioxide.* Journal of Chemical Engineering of Japan, 1997. **30**(2): p. 293-301.

23. Shim, J.-J., Yates, M.Z., Johnston, K.P., *Polymer coatings by rapid expansion of suspensions in supercritical carbon dioxide.* Ind. Eng. Chem. Res., 1999. **38**: p. 3655-3662.

24. Kwauk, X. and P.G. Debenedetti, *Mathematical Modeling of Aerosol Formation by Rapid Expansion of Supercritical Solutions in a Converging Nozzle.* J. Aerosol Science, 1993. **24**(4): p. 445-469.

25. Ksibi, H. and P. Subra, *Influence of Nozzle Design on the Nucleation Conditions in the RESS Process.* Chem. Biochem. Eng. Q., 1996. **10**(2): p. 69-73.

26. Franklin, R.K., et al., *Formation of Perfluoropolyether Coatings by the Rapid Expansion of Supercritical Solutions (RESS) Process Part 2: Numerical Modeling.* Industrial & Engineering Chemistry Research, 2002.

27. Bungert, B., G. Sadowski, and W. Arlt, *Separations and Material Processing in Solutions with Dence Gases.* Ind. Eng. Chem. Res., 1998. **37**: p. 3208-3220.

28. Larson and King, *Evaluation of Sipercritical Fluid Extraction in the Pharmaceutical Industry.* Biotechnology Progress, 1986. **2**(2): p. 73-82.

29. Chernyak, Y., et al., *Formation of Perfluoropolyether Coating by the Rapid Expansion of Supercritical Solutions (RESS) Process*
Part 1: Experimental Results. Industrial & Engineering Chemistry Research, 2002. **40**(23): p. 6118-6126.

30. Bunyard, W.C., *Novel methods for synthesis of perfluoropolyethers*. 2000, University of North Carolina at Chapel Hill.

31. Altunin, V.V. and O.G. Gadetskii, *Equation of State and Thermodynamic Properties of Liquid and Gaseous Carbon Dioxide.* Tepolenergetika, 1971. **18**(3): p. 81-84.

32. NIST, N.I.o.S.a.T.-. *NIST Standard Reference Database Number 69*. 2001.

33. Heertjes, P.M. and N.W.F. Kossen, *Measuring the Contact Angles of Powder-Liquid Systems.* Powder Technology, 1967(1): p. 33-42.

34. Davies, J.T. and E.K. Rideal, *Interfacial Phenomena*. 1963, London: Academic Press, INC.

35. Kossen, N.W.F. and P.M. Heertjes, *The determination of the contact angle for systems with a powder.* Chemical Engineering Science, 1965. **20**: p. 593-599.

36. Pereira, C.P., R.W. Rice, and J.P. Skalny. *Pore Structure and its Relationship to Properties of Materials*. in *Mat. Res. Soc. Symp. Proc : Pore Structure and Permeability of Cementitious Materials*. 1989. Pittsburgh, PA: MRS.

37. Bird, R.B., W.E. Stewart, and E.N. Lightfoot, *Transport Phenomena*. 1960: John Wiley & Sons. 502.

38. Geankoplis, C.J., *Transport Process and Unit Operations*. Third ed. 1993: Simon & Schuster. a)464, b)462, c)463, d)395.

39. Dullien, F.A.L., *Porous Media - Fluid Transport and Pore Structure*. Second ed. 1992, San Diego, California: Academic Press, Inc.

6. Appendices

6.1 RESS Operational Procedure

Brief Description of Process

This operating procedure covers the use of Rapid Expansion of Supercritical Solutions (RESS) apparatus and significant safety precautions. The apparatus is set-up for expansion of supercritical polymer/CO2 solutions to ambient condition. The process temperature range is from 20° C to 120° C and pressure range is up to 7000 psi.

Significant Safety Precautions

- Wear safety glasses with side shields and cotton lab coat during the RESS apparatus operation or other activities in the lab
- Wear leather gloves when working with tools and handling cylinders
- Wear Kevlar ® gloves when handling glass
- Use the proper gloves for handling the sample (refer to MSDS or cross-reference)
- Keep the hood sashes closed during the measurements

Description of the apparatus

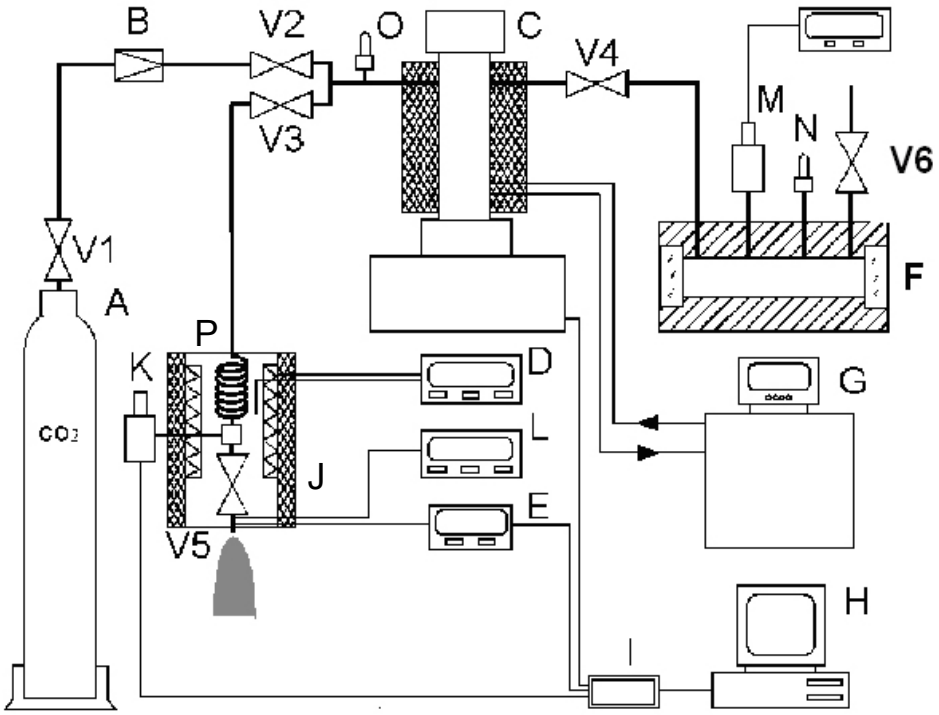

Figure 6.1.1: RESS apparatus

The experimental setup is shown schematically in Figure 1. Solution of polymer in CO2 is prepared at ambient temperature in the extraction cell **F**. Extraction cell **F** is a high-pressure stainless steel cell with sapphire windows. Then polymer/ CO2 solution is pressurized by the ISCO syringe pump **C** and is heated to the desired starting process conditions (P_{exp} and T_{exp}). The temperature of the solution in the syringe pump is regulated by circulating water/ethylene glycol mixture from the thermostated bath **G**.

To initiate the RESS precipitation, the solution is pumped at pressure P_{exp} to the pre-expansion unit **J** and is heated isobarically to the pre-expansion temperature Ts by

passing it through the heated coil leading to a nozzle. In the nozzle the supercritical solution is allowed to expand to ambient pressure. The temperature Ts of the pre-expansion unit is controlled by Omega temperature controller **D** and is maintained constant all the time during solution expansion in the nozzle. The pressure and temperature is measured upstream of the nozzle orifice by Omega pressure transducer **K** and K-type thermocouple **E**, receptively.

A PC based data acquisition system (DAS) records and stores all measured parameters (i.e. pressure, temperature, flow rate). The main components of DAS are the analog/digital conversion system OMEGA CIO-DAS08 **I** and process computer Gateway 2000 **H**.

Summary of the experimental uncertainties

Pressure	Temperature	Flow rate	Concentration
Pressure transducer $\Delta P1$= 100 psi	Thermostated bath ΔTe= 2 K	Syringe pump ΔQ= 0.5% (0.5 ml/min)	Analytical balances Δm polymer= 0.001g
Pressure readout $\Delta P2$= 1psia @ P=5000 psi	K-type thermocouple and temperature readout $\Delta Ts1$= 2.4 K	Pump analog output ΔQ= 1% (1 ml/min)	Syringe pump $\Delta Vco2$= 0.03ml
DAS $\Delta P3$= 2.5 psi	Temperature controller $\Delta Ts2$= 2.6 K	DAS ΔQ=0.25 ml/min	Syringe pump $\Delta m\ co_2$= 0.001g
	DAS $\Delta Ts3$= 0.25 K		
Total ΔP= 101 psi	Total ΔTe= 2 K Total ΔTs= 3.6 K	Total ΔQ= 1.15 ml/min	Total $\Delta W = 10^{-5}$

List of the equipment used

Equipment/ Instrumentation Model	Pressure Rating	Working Temperature	Material	Capacity/ Size	Supplier
ISCO 260D Syringe Pump	7,500 psi	-50 to 100 °C	316 Stainless Steel	266 ml	ISCO, Inc.
Omega Pressure Transducer Model PX302-10KGV	10,000 psi	-18 to 71 °C	316 Stainless Steel	1/4" NTP	OMEGA
Omega Digital Panel Meter Model DP25	N/A	Ambient	N/A		OMEGA
Extraction Cell	X,000 psi	@ 25 °C	316 Stainless Steel	110 ml	NCSU machine Shop
Sapphire Windows	X,000 psi	@ 25°C	Sapphire	diameter X/4", thickness X/4"	
Thermostated Bath RC 20	N/A	-30 to 150 °C	N/A	2 l	Lytron, Inc.
Rupture Disk	8,500 psi	@ 25 °C	316 Stainless Steel	1/4"	High Pressure Equipment
Ball Check Valve	10,000 psi	@ 25°C	316 Stainless Steel	1/4"	High Pressure Equipment
K-type Thermocouple CASS-116(G)-12	N/A	-200 to 1250°C	304 Stainless Steel chrome ga/al omega	1/16" diameter 12" length	OMEGA
Omega Temperature Controller CN76000	N/A	-129 to 990 °C	N/A		OMEGA
Heating Tape	N/A	-X0 to X0 °C		X" length X" width	

List of the equipment used (Continued)

Analytical Balance AB204	N/A	N/A	N/A	250 g	Metter Toledo
Equipment/ Instrumentation Model	Pressure Rating	Working Temperature	Material of Construction	Capacity/ Size	Supplier
Valves	15,000 psi 15,000 psi 10,000 psi	@ 25 °C " "	316 Stainless Steel " "	1/16" 1/8" 1/4"	High Pressure Equipment
Tubing	15,000 psi 15,000 psi 10,000 psi	@ 25 °C " "	316 Stainless Steel " "	1/16" 1/8" 1/4"	High Pressure Equipment
Fittings	10,000 psi	@ 25 °C	316 Stainless Steel	vary	High Pressure Equipment
CO2 cylinder Bone Dry Grade purity 99.XX %	860 psi	@ 20 °C	316 Stainless Steel	standard	National Welders
Analog/Digital Interface CIO-DAS08	N/A	N/A	N/A		OMEGA
Computer	N/A	N/A	N/A		Gateway

Preparation of System

Refer to Figure 1 for schematic information.

1 Loading polymer

1.1 Determine the amount of polymer needed to produce a pre-determined weight percent solution from the following equation:

$$m_{polymer} = \frac{wt\% \cdot m_{CO_2}}{1 - wt\%} \qquad (1)$$

Note: for this particular system a relatively constant amount of liquid CO_2 can be collected in the ISCO pump to make the CO_2/polymer solution. At 4000 psi and 10 degrees C it is approximately 230 cc which correlates to 232 grams of CO_2 at that temperature and pressure

1.2 Put the desired amount of polymer into a syringe and record the weight

1.2.1 Either weigh the syringe before polymer is loaded, or place the empty syringe on the balance and zero the weight. This will allow accurate measurement of the polymer mass. If it is decided to zero the balance, ensure that the balance is not reset during the loading process.

1.3 Remove 1/8th inch fitting on top of the view cell and inject polymer into cell

1.4 Weigh the syringe, the difference between the two readings is the polymer deposited in the system. Now the wt% can be calculated from equation 1

1.5 Flash CO_2 into the view cell removing the air.

1.5.1 Valves V1 and V2 should be open

1.5.2 Crack open valve V4 and close immediately

Note: This allows CO_2 from the cylinder to flow into the view cell and forces out the air that is in the view cell

1.5.3 Replace the $1/8^{th}$ inch fitting on top of the view cell approximately 5 to 10 seconds after cracking open valve V4

2 Mixing Solution

2.1 Turn on equipment: pressure transducer, temperature readout, and magnetic stirrer

2.2 Set the thermostated bath to a temperature of 10 degrees C

2.3 Check that valves V1 and V2 are open

2.4 Fill ISCO pump with CO_2

2.4.1 After the ICSO pump is full keep valves V1 and V2 open for at least 30 minutes

Note: At 10 degrees C the pump will continue to collect liquid CO_2 over this time

2.5 Close valve V2

2.6 Set pressure of ISCO pump to maintain 4000 psi

Note: 4000 psi was chosen as it is well above the cloud point curve for the polymers used for experimentation also volume of liquid CO_2 should be approximately 230 cc

2.7 Set the thermostated bath to a temperature of 23 degrees C (room temperature)

2.8 Open valve V4 to mix liquid CO_2 and polymer.

Note: Allow the polymer to dissolve this takes anywhere from 15-30 minutes. The progress can be checked through the sapphire window. When the polymer is completely dissolved the solution will be clear.

2.9 Use the "fill" option on the ISCO pump to draw the solution out of the view cell into the ISCO pump

2.10 Set the ISCO pump back to 4000 psi.

2.11 Allow the polymer to dissolve once again and repeat this process 2 more times.

Note: Steps 2.9 through 2.11 are used to mix the solution

2.12 Allow the system to remain at 4000 psi and 23 degrees C overnight

Note: This is to ensure that all of the polymer is dissolved and equilibrium of solution concentration is reached between the viewing cell and the ISCO pump

3 Spraying

3.1 In the morning check system for leaks and close valve V4

3.2 Turn on equipment: temperature controllers

3.3 Check that valve V5 is closed and open valve V3

3.4 Set the desired temperature for spraying on the thermostated bath and the temperature controllers

3.5 Set the desired pressure for spraying on the ISCO pump

3.6 Wait at least 30 minutes for the system to reach equilibrium

Note: It may take longer for the temperature to reach desired point. It has been observed during setup that there is a significant delay in heat transfer from the heating tape to the thermocouple. This results in an over heating of

the heating tape before the temperature controller regulates the heating tape. The best technique devised for this system is to monitor the temperature of the heating tape and allow it to overshoot the desired temperature and then manually turn it off. The higher the process temperature the higher the over shoot may be allowed. For example when setting process conditions of 40 degrees C, the heating tape is allowed to reach a temperature around 80 degrees C before turning off. Now monitor the temperature of the heating tape, when it reaches the desired temperature turn on the temperature controller. The temperature of the thermocouple will now be displayed. If the temperature is still not to the desired position continue the process. The process becomes more fined tuned only through first hand experience.

3.7 Turn on data acquisition system and exhaust fan

3.8 Open valve V5 to expand polymer solution through nozzle

4 Normal Shutdown

4.1 Open V6 to vent view cell

4.2 Check that valve V1 is closed and open all other valves

4.3 Turn off equipment: exhaust fan, data acquisition, temperature controllers, thermostated bath, pressure transducer

Cleaning RESS device

5 Cleaning ISCO pump and lines

5.1 Close valves V3, V4, V5,V6

5.2 Open valves V1, V2 and open regulator on CO_2 cylinder

5.3 Set Temperature on the thermostated bath to 10 degrees C

5.4 Fill ISCO pump with CO_2

5.4.1 After the ICSO pump is full keep valves V1 and V2 open for at least 30 minutes

Note: At 10 degrees C the pump will continue to collect liquid CO_2 over this time

5.5 Close valve V2

5.6 Set pressure of ISCO pump to maintain 4000 psi

Note: 4000 psi was chosen as it is well above the cloud point curve for the polymers used for experimentation

5.6.1 Allow pump to remain at this pressure for at least 30 minutes and check for leaks

Note: This allows the liquid CO_2 to dissolve any polymeric material remaining in the pump from previous runs

5.7 Open valve V3

5.7.1 Allow system to remain at this pressure for at least 30 minutes and check for leaks

Note: This allows the liquid CO_2 to dissolve any polymeric material remaining in the pump and line of the system

5.8 Turn on exhaust fan

5.9 Open valve V5

5.9.1 Allow all of the CO_2 to leave the system

5.10 Repeat all of the above steps two additional times.

5.11 Close valves V3 and V5

5.12 Turn off exhaust fan

6 Cleaning view cell

Note: This process can be completed during the CO_2 flushing of the system described in section 1

6.1 Check valve V4 to be sure it is closed

6.2 Open valve V6 to vent any pressurized solution in the view cell

6.3 Once the pressure in the view cell has been relieved, remove the sapphire windows and O-rings on each side

6.4 Remove magnetic stir bar

6.5 Spray acetone inside view cell and pass an acetone soaked lint free tissue through the cell, next wipe dry with lint free tissue

Note: organic solvents such as acetone are very good solvents for the polymer used for this experimentation

6.6 Clean sapphire windows, O-rings, fittings, and magnetic stirrer with acetone and wipe dry with lint free tissues

6.7 Replace magnetic stirrer, then replace sapphire windows and secure fittings

7 Emergency Shutdown

7.1 Turn off all instruments. Open valve V3 and close other valves

6.2 Online Particle Sizing Operation

NOTE: The Malvern Spraytec Model RTS 5006 particle sizing system has a software manual that will explain some of the menus more in depth. This outline provides a step by step guide to the operational procedure used during this experimentation.

1. Open RTSizer program

1.1. Turn on computer and power supply to the Malvern Spraytec Model RTS 5006 droplet sizing system.

1.2. "Double click" on RTSizer program icon.

2. Adjusting Measurement Settings

2.1. From the main screen select the "Edit" pull down menu

2.1.1. Select "Access level" option

2.1.1.1. There will be a prompt for password, upon instillation of the software a password was not set therefore no password is required to change access level

2.1.1.2. Select Ok

2.1.1.3.The Access level should be set to level 2 now. Some options are not available unless a higher access level is set.

2.2. From the main screen select the "Edit" pull down menu

2.2.1. Select "Reduction control" option

2.2.1.1. Select Reduction control tab

2.2.1.1.1. First Scattering Ring is set to 21, which corresponds to 10.34 μm

2.2.1.1.2. Last Scattering Ring is set to 31, which corresponds to 1.5 μm

NOTE: This does not turn off the detection rings that are not selected this option displays readings from only the rings selected. It is possible to change this setting after an experiment and view the additional data.

2.3. All other parameters should remain at their default settings

2.4. Once settings are changed they will remain at changed values even when the program is closed

3. Data Acquisition

3.1. For each experimental run it is advised to start a new data file

3.2. From the main screen select "File" then "New" then "Time History File". This will open a new time history data file.

3.3. There are three windows displayed on the time history file, all of which are configurable.

3.3.1. The main window occupies the lower half of the screen. This is the time history plot. To set the display, "right click" inside the window and select "display settings"

3.3.1.1.Select "view 7" tab: this view provides a tracking of transmission, Dv(90), Dv(50), and Dv(10). In addition the display settings, allows you to set the display limits for transmission and diameter. For this

experiment the transmission limits were 100 upper and 0 lower. The diameter limits were 20 upper and 0 lower.

3.3.1.2. To set this view "right click" once more on the time history window and select "View 7: Size vs. Transmission". This will place a check beside the selection.

3.3.2. The top half of the screen is split between two windows. Each have the option to display the following plots: PSD(Particle Size Distribution), Corrected Scattering, Raw Scattering, and Background. The windows may also display a cover page that displays information about the time history file such as date, time, recorded values, etc. To switch between these views, "right click" inside the window and select the desired view. For this experimentation the PSD graph and the cover page were chosen to display.

3.3.3. The settings of the PSD graph may be changed by "right click" on the plot window. It is necessary to adjust the graph limits for proper display of the results. The lower size is set to 0.1 and the upper to 100. The volume frequency is set to a maximum of 50%.

3.4. Located on the bottom left side of the Time History display there are four buttons: "start", "tag", "update", and "background"

3.4.1. select "Tag"

3.4.1.1. Enter the material used in the experiment (ie. UNC diamide 2 wt%)

3.4.1.2. Enter the temperature and pressure of the syringe pump and temperature of the nozzle in the "notes" section

3.4.1.3. This information on the experimental run is stored on the time history file so that upon later data examination the process conditions will be known.

3.4.1.4. Close Tag section

3.4.2. Select “Background”.

3.4.2.1. This process is a calibration of the background noise registered by the detection rings. It is now necessary to turn off the overhead lights and any light source near the experimental setup. Also the blinds on the windows should be lowered and closed. The system is particularly sensitive to sunlight.

3.4.2.2. Select “Ok”. The system will begin a 5 second calibration reading.

3.4.2.3. A plot of the signal results will be displayed after the 5 second calibration. The center ring, (ring 0) should have a transmission reading of approximately 1500. The remaining rings should display a scattering signal below 50. If the transmission signal is low or if the scattering signal is high the lens of the system should be cleaned.

3.4.2.3.1. To clean: First turn off the power supply, this is to avoid accidentally looking into the laser beam. With a lab wash bottle spray the lens with acetone and wipe dry with a lint free tissue. The acetone should evaporate rather quickly. When the lenses are dry turn power supply on and repeat steps 4.3.2 through 4.3.2.3.

3.4.2.3.2. If the background results remain outside acceptable readings repeat cleaning and insure there is no residue on the lenses. If a

problem continues there could possibly a misalignment of the laser. If this is suspected, the technical manuals should be consulted and appropriate steps followed.

3.4.3. Select “Start”

3.4.3.1. The system is calibrated and the RESS system should be ready to spray. The lights in the laboratory should remain off during the experiment.

3.4.3.2. Once the “Start” button is selected a messaged will be displayed: “Configure the values for PSD measurement”. Select “Ok”.

3.4.3.3. Data acquisition will begin. If the system has been calibrated properly the system should register no reading. If this is the case a solid blue band will appear in the time history plot. If this is the case continue to 4.4.3.4.

3.4.3.3.1. If the system detects particles, there are two possible causes. This first, background calibration is off. This could possible be from an increase in sunlight penetrating the window blinds. The window blinds do not completely block out all the light. This has been observed during experimentation. To resolve, select the “stop” button and perform another background measurement. The second cause is that dust has been stirred into the air. The laboratory area is not clean, and dust can easily be stirred into the air. To resolve, select the “stop” button and wait for dust to settle.

If the problem persists after trying the two remedies, it might be indicative of an alignment problem.

3.4.3.4. The system is not detecting particles. Open the nozzle valve on the RESS system. Now a real time display of particle size distribution as well as Dv(90), Dv(50), Dv(10) and Transmission will be displayed.

3.4.3.5. Monitor the volume remaining ISCO Syringe pump. Data acquisition should be stopped before the contents of the pump are emptied. Select "stop" when the pump is nearing empty.

4. Data Processing

4.1. Upon completing an experiment it is necessary to judge whether the data is useful. Below in figures 4.1 and 4.2 two time history plots are shown. The plots display particle diameter measurements: Dv(90), Dv(50), Dv(10) and Transmission (T). The solid bands represent no detectable particles. The first plot (figure 4.1) displays readings that are relatively constant for all values. This was a stable experiment from beginning to end.

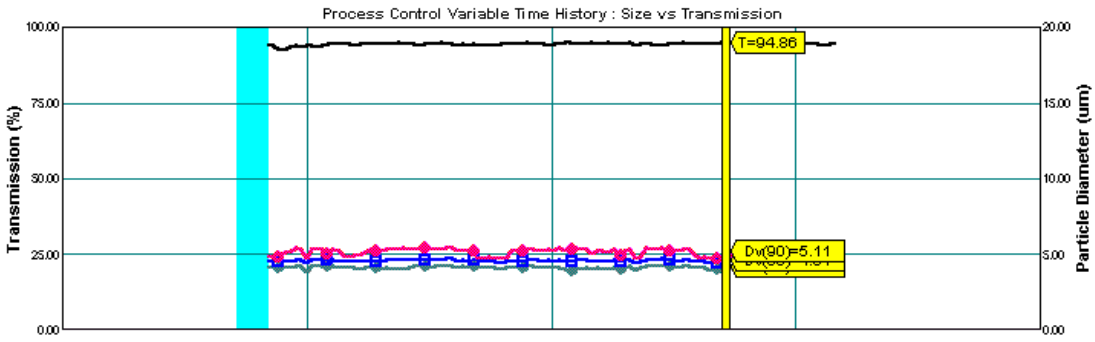

Figure 6.4.1: Time history plot

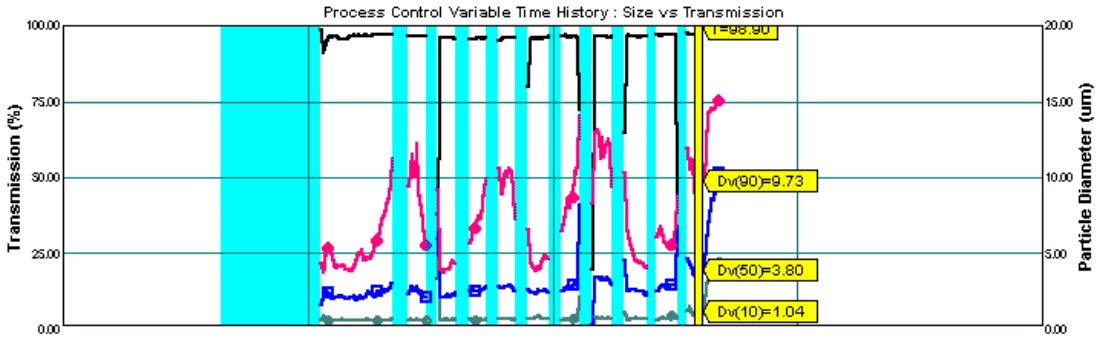

Figure 6.4.2: Time history plot

Figure 4.2 displays an experiment where no useful data is recorded. It can be seen that readings are not stable and there is a periodic occurrence where no particles are detected. There was not an error in data acquisition for this particular experiment.

The flow never stabilized over the course of the experiment. It was observed during experimentation that in some cases the spray will require a short period of time to stabilize. The stabilization usually occurs within 15 seconds.

4.2. Once it is determined that the run was stable, it is necessary to calculate an average of the particle size distribution.

4.2.1. Highlight the duration of readings that are to be averaged. This is done by "left click and drag" on the time history window.

4.2.2. From the main menu select the "Calculate" then "Average" this will bring up an option window that prompts for: range, screen or all. Select "range" to average the highlighted region and the click "ok". The other two options are used if you wish to average the entire data record, or the record currently displayed on the screen.

4.2.2.1. If the “Average” option is not available, then the access level must be changed. This is done exactly as before. Select “Edit” then “Access level” then “Ok”. Again no password is required.

NOTE: It was observed during experimentation that the software would not average the time history plot. If this occurs then the program must be closed and opened again. Be sure that the data file is saved before closing the program. If the problem persists, then restart the computer. These two solutions fixed the software bug each time it occurred during experimentation. If the problem is still present after trying the two solutions it is necessary to contact technical support from Malvern/Insitec.

4.2.3. Now an average particle size distribution (PSD) will be displayed on the screen.

4.2.4. Its display settings can be changed by using “right click” as described above

4.3. Once the desired display is set print the averaged PSD display and cover page

4.3.1. Select from the main menu “File” then “Print”. An option window will appear where plots can be selected to print.

4.3.2. “Left click” to check the plots to print. For most cases this will be the PSD and Cover page. Select “Ok” to begin printing.

4.3.2.1.The cover page provides numerical displays of the averages calculated as well as experimental documentation such as: date, time, etc.

4.3.3. To print the time history plot, select the time history window. This is done by simply "left click" anywhere on the window.

4.3.4. Select "File" then "Print". An option window similar to the one for calculating averages will appear. Select the option desired and the select "Ok"

NOTE: It was observed during experimentation that the software would not print the time history plot. If this occurs then the program must be closed and opened again. Be sure that the data file is saved before closing the program. If the problem persists, then restart the computer. These two solutions fixed the software bug each time it occurred during experimentation. If the problem is still present after trying the two solutions it is necessary to contact technical support from Malvern/Insitec.

4.4. It is possible after the experiment to change the data that is displayed. As noted before, data is collected by all the detection rings even though their display is turned off.

4.4.1. To change the settings Select "Edit" then "Records". This will open an option window similar to that for calculating the average. It may be necessary to change the access level to have this option available.

4.4.2. The option window will allow you to select all of the data or a specified section. To select a section to alter highlight the desired section just as done for calculating the PSD average.

4.4.3. After selecting the section to change an menu will pop up that displays: "Tag", "Process variables", "Background", and "Reduction Control". "Left

click" on any of these menus will allow you to change setting previously specified. For most purposes this will not be necessary. For instance the particle size limits may be changed under "Reduction control" by changing the detector rings that are displayed.

5. Saving and File Documentation

5.1. Select "File" then "Save". Then simply enter a name for the data file and location on the computer to save.

5.2. Now a log entry is filled out using a text editor program (ie. WordPad or Microsoft Word) on the computer. An example of a log entry is shown below. The log is printed and filed with the other print outs to provide a detailed record of the experiment.

NOTE: It is necessary to record operational conditions during the experiment, such as Pressure (P) and flow rate (Q). It is possible for one person to operate the data acquisition program and record this data, although with two people this is easier to monitor the experiment.

Sample Log Entry

Date: 4-03-2001

Data File: Apr3a_2001.pcl

Material: UNC diamide

Conditions:

Composition: ~ 2.0 %

P = 2400 psi

T(pump) = 25 C

T(pre expansion) = 26 C

T(line) = 26-24

Q = ~39 ml/min

Nozzle: L = 25 mm capillary nozzle # 3

NOTES: very uniform flow, it stabled out very quickly